https://doi.org/10.1070/RCR4965

Recent advances in chemistry of high-spin nitrenes

Sergei V. Chapyshev,* Denis V. Korchagin, Evgenii Ya. Misochko

Institute of Problems of Chemical Physics, Russian Academy of Sciences, prosp. Akademika Semenova 1, 142432 Chernogolovka, Moscow Region, Russian Federation

Experimental and theoretical studies on aromatic nitrenes bearing from three to six unpaired electrons and having quartet, quintet, sextet or septet ground spin states, published in the last 15 years are analyzed. A comparative analysis of the magnetic properties of high-spin nitrenes and all other known high-spin organic molecules is performed. Promising areas of practical application of high-spin nitrenes as molecular magnets and as qubits and qudits for quantum computations are discussed. The bibliography includes 214 references.

Contents

1. Introduction 39
2. Historical survey 39
3. Magnetic parameters of high-spin molecules 41
4. High-spin nitrenes with *sym*-triazine skeleton 42
5. High-spin pyrimidinylnitrenes 44
6. High-spin pyridylnitrenes 44
   6.1. Quintet pyridyldinitrenes 44
   6.2. Septet pyridyltrinitrenes 45
7. High-spin nitrenobenzenes 47
   7.1. Quintet *m*-phenylenedinitrenes 47
   7.2. High-spin oligoarylnitrenes 48
   7.3. Septet trinitrenobenzenes 50
8. High-spin nitrenocarbenes and nitreno radicals 53
9. Nitrenes and other high-spin organic molecules: a comparison 55
   9.1. Main spin units 56
   9.2. Spin – spin interactions in triplet diradicals 56
   9.3. Spin – spin interactions in quintet tetraradicals 58
   9.4. Spin – spin interactions in septet hexaradicals 59
   9.5. Organic polyradicals with $S > 3$ 59
10. Quantum chemical calculations of high-spin nitrenes 61
   10.1. Calculations of IR spectra, geometric parameters and spin density 61
   10.2. Calculations of UV spectra 61
   10.3. Calculations of zero-field splitting parameters 62
11. Possible application fields of high-spin molecules 63
12. Conclusion 65

1. Introduction

Most organic molecules have paired electrons and a singlet ground spin state ($S = 0$), which implies only one energy minimum for a molecule irrespective of the presence of external magnetic field. Organic molecules bearing one unpaired electron have a doublet ground spin state $S = 1/2$, since in external magnetic field the lowest-lying energy level of these molecules is split into two sublevels with spin orientation along and opposite to the external magnetic field (Zeeman effect).[1] In molecules bearing two unpaired electrons each of them is in the magnetic field induced by the adjacent electron. Therefore, splitting of the lowest-lying energy level in such molecules into three sublevels occurs in the absence of external magnetic field and is termed zero-field splitting (ZFS), the molecules being called triplet states ($S = 1$). Molecules with three, four, five and six unpaired electrons have the spin states $S = 3/2$, 2, 5/2 and 3, respectively, and are termed quartet, quintet, sextet and septet ones.[1] Under the action of external factors, such molecules can change their magnetic moments, spin populations of energy sublevels and the spin state, thus being of considerable interest as molecular devices for spintronics and quantum informatics.[2–20] This review is devoted to recent advances in the synthesis and studies on the properties of a class of high-spin organic molecules, *viz*., aromatic nitrenes with the quartet, quintet, sextet or septet ground spin states. Chemistry of triplet arylnitrenes has been well documented in reviews[21–29] and monographs.[30–35] The results of the early studies on quintet dinitrenes were summarized elsewhere.[36–39]

2. Historical survey

The existence of organic nitrenes (monovalent nitrogen compounds) was for the first time demonstrated in 1962 by researchers from Bell Telephone Labs, Inc. (USA), who detected a number of signals in the EPR spectra of several triplet mononitrenes generated during the photolysis of organic azides in frozen organic solutions at 77 K.[40] More recently, researchers from the same group reported the

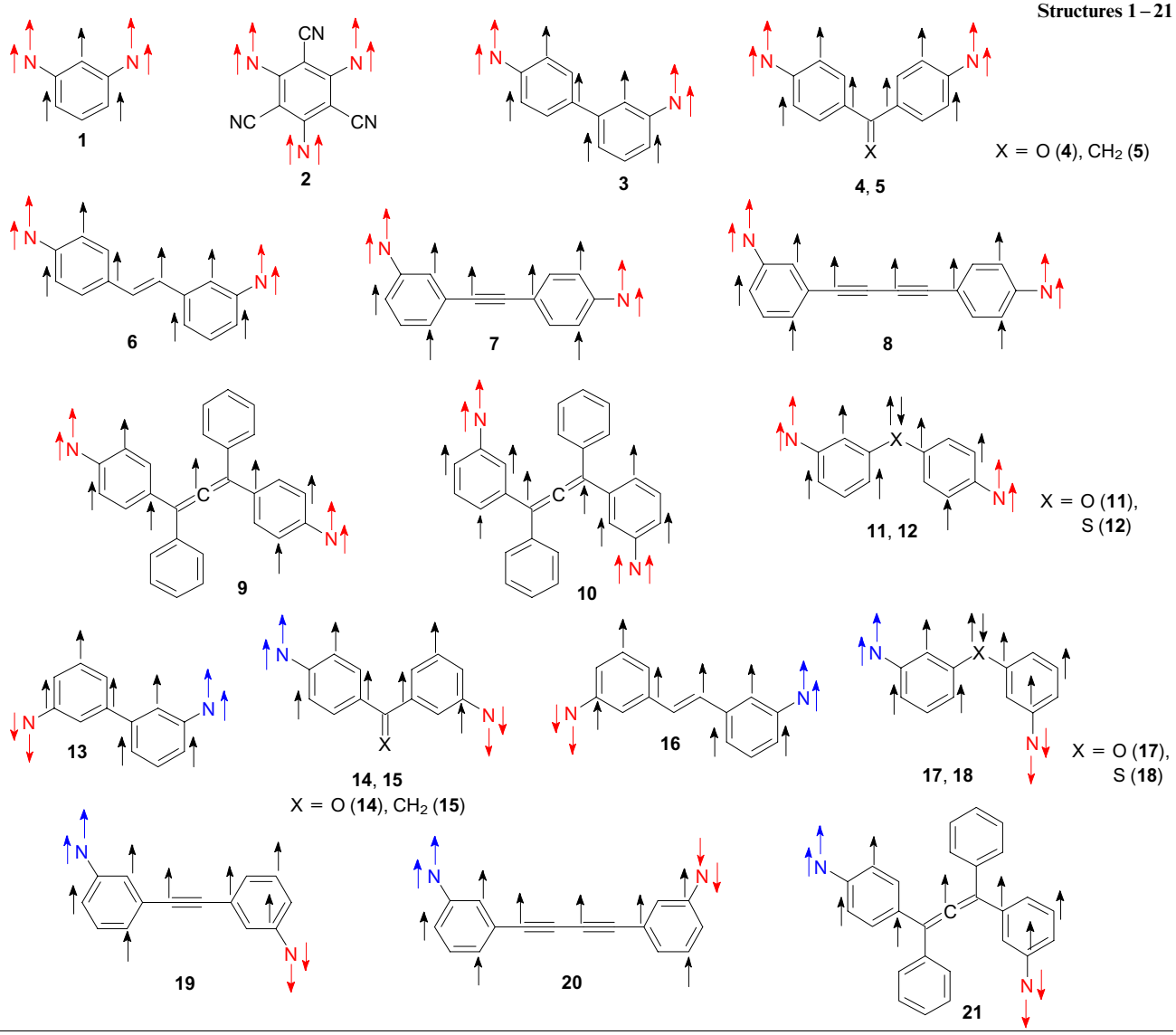
S.V.Chapyshev. Doctor of Sciences (Chemistry), Principal Researcher at IPCP RAS.
Telephone: +7(496)522–1532, e-mail: chap@icp.ac.ru
Current research interests: chemistry of aromatic polyazides and high-spin nitrenes.
D.V.Korchagin. Candidate of Sciences (Chemistry), Leading Researcher at IPCP RAS.
Telephone: +7(496)522–1531, e-mail: korden@icp.ac.ru
Current research interests: single-molecule magnetism, quantum chemical calculations of the structure and properties of high-spin molecules, magnetic anisotropy, spin – orbit effects.
E.Ya.Misochko. Doctor of Sciences (Physics and Mathematics), Head of Laboratory at IPCP RAS.
Telephone: +7(496)522–1280, e-mail: misochko@icp.ac.ru
Current research interests: radical intermediates, high-spin molecules, molecular magnets, EPR spectroscopy.

Translation: A.M.Raevskiy

Received 26 May 2020

© 2021 Uspekhi Khimii, ZIOC RAS, Russian Academy of Sciences and IOP Publishing Limited

Structures 1–21



detection of the EPR spectra of quintet dinitrene **1** and septet trinitrene **2**.[41,42] However, the ZFS parameters of these nitrenes remained unknown for long since no software for processing complex EPR spectra of high-spin nitrenes was available. Nevertheless, the generation of nitrenes **1** and **2** gave an impetus to intensive EPR studies of various aryldinitrenes.[36,37]

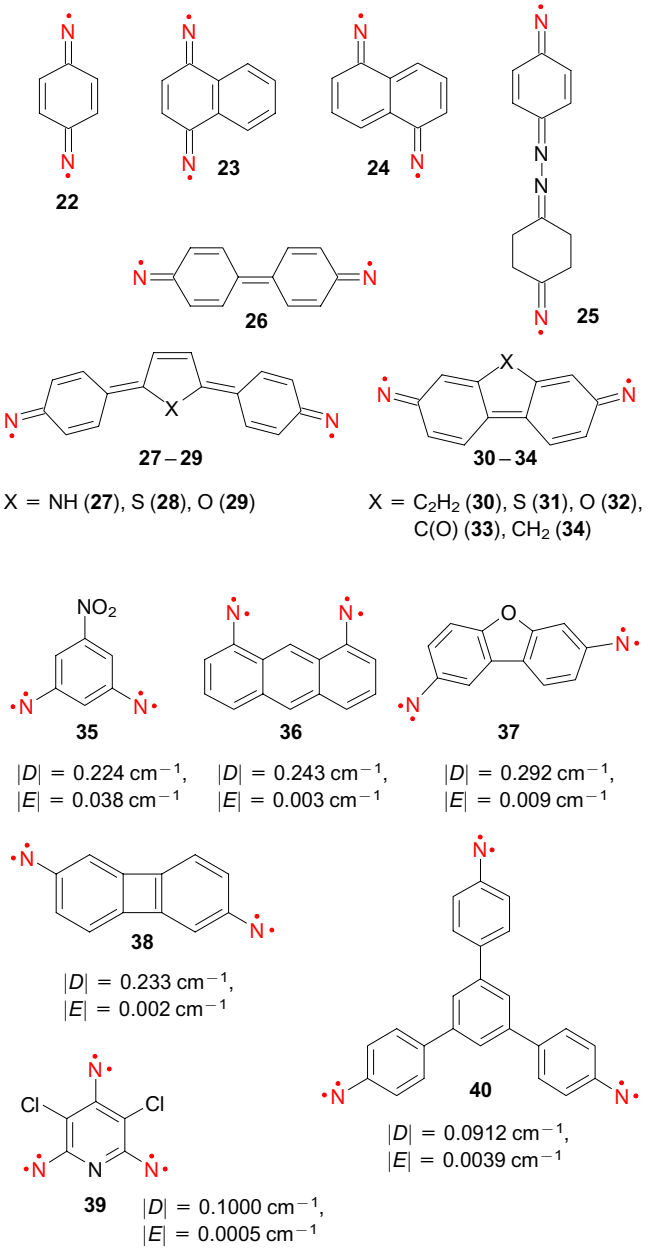
It was found that all aryldinitrenes can be divided into three classes, *viz.*, nondisjoint, disjoint and quinonoid dinitrenes.[36,37] Examples of nondisjoint aryldinitrenes are provided by compounds **1** and **3**–**12**. In the spin-polarized π-systems of these dinitrenes, the numbers of alternating atoms with the α- and β-spin density are respectively denoted as n^* and n^0 and obey the condition $n^* > n^0$. Such an alternation of the α- and β-spin density ensures a parallel orientation of spins on nitrene centres of dinitrenes **1** and **3**–**12** and a quintet ground spin state, which lies 10–20 kcal mol^{-1} lower than the excited triplet states. The intensities of the EPR signals of quintet dinitrenes **1** and **3**–**12** obey the Curie law, that is, increase linearly as temperature decreases.

Disjoint aryldinitrenes can be exemplified by compounds **13**–**21**.[36,37] Molecules of these dinitrenes have $n^* = n^0$, oppositely oriented spins at the nitrene units and a singlet ground spin state lying merely 100–800 cal mol^{-1} lower than the excited quintet states. In the EPR spectra, dinitrenes **13**–**21** appear as signals of excited quintet molecules; the signal intensities do not obey the Curie law.

Compounds **22**–**34** represent quinonoid aryldinitrenes.[36,37] They have a singlet ground spin state, although their EPR spectra exhibit signals from excited triplet biradicals.

The development of software for calculating the EPR spectra of high-spin molecules with strong magnetic anisotropy in 1996 offered new prospects for research on nitrenes.[43] It took a short time to exactly determine the ZFS parameters of structurally highly dissimilar quintet dinitrenes **35**,[43] **36**, **37** (Ref. 44) and **38**,[45] as well as those of two septet trinitrenes **39** (Ref. 46) and **40**.[47] However, the greatest progress in the studies of high-spin nitrenes was made in the last 15 years owing to the use of high-frequency W-band EPR spectroscopy (~94 GHz) and X-band EPR spectrometers operating at about 9.5 GHz and equipped to work with argon matrices, as well as to the development of software for simulation of EPR spectra and quantum chemical calculations of the ZFS parameters of high-spin

Structures 22 – 40



molecules.[48, 49] The main achievements made during this period of research into high-spin nitrenes are considered below.

3. Magnetic parameters of high-spin molecules

In the absence of external magnetic field the interaction between unpaired electrons causes the lowest-lying energy level of molecules with $S > 1/2$ to split into $2S+1$ sublevels (fine-structure energy levels). This ZFS effect is described by the spin Hamiltonian (1)

$$\boldsymbol{H}_{S=n} = D\left[S_z^2 - \frac{1}{3}S(S+1)\right] - E(S_x^2 - S_y^2) \qquad (1)$$

where S_z, S_x and S_y are the components of the spin angular momentum of the system along the Z, X and Y axes, respectively; $D = (3/2)z$; $E = (1/2)(x-y)$; and x, y and z are the eigenvalues of the ZFS tensor in the system of principal axes X, Y and Z ($x + y + z = 0$ and $|z| > |x|$ and $|z| > |y|$).[1] At $x = y$, the spin system has a cylindrical symmetry, and one has $E = 0$. The magnetic parameters D and E characterize the energy intervals between the fine-structure energy levels in the approximation of dipole – dipole spin – spin interactions and are inversely proportional to the cubed distance between the unpaired electrons.[21, 25]

In external magnetic field H, the spin Hamiltonian of high-spin molecules with the spin angular momentum S has the form

$$\mathrm{H} = g\beta HS + \mathrm{H}_{S=n} \qquad (2)$$

where g is the g-factor ($g \sim 2$) and β is the Bohr magneton.

For quintet molecules with $E = 0$, the zero-field splittings between the energy sublevels W_0, $W_{\pm1}$ and $W_{\pm2}$ are approximately equal to $W_{\pm1} - W_0 = |D|$ and $W_{\pm2} - W_{\pm1} = |3D|$.[1] For septet molecules with $E = 0$, the system of sublevels W_0, $W_{\pm1}$ and $W_{\pm2}$ is augmented with the sublevels $W_{\pm3}$ characterized by $W_{\pm3} - W_{\pm2} = |5D|$.[1] If $E \neq 0$, each of the sublevels $W_{\pm1}$, $W_{\pm2}$ and $W_{\pm3}$ is split by $2E$. In an external magnetic field, the sublevels W_0, $W_{\pm1}$, $W_{\pm2}$ and $W_{\pm3}$ of high-spin molecules are split into the sublevels W_{+3}, W_{+2}, W_{+1}, W_0, W_{-1}, W_{-2} and W_{-3} and the higher the external magnetic field the larger the splitting.

The magnetic parameters D and E of high-spin molecules are experimentally determined using EPR spectroscopy. First-order EPR spectra of quintet molecules with $E = 0$ demonstrate two sets of four lines corresponding to single-photon XY and Z transitions ($\Delta m_s = 1$) with the centre of symmetry at $g = 2$.[1] Spectral lines corresponding to the Z transitions are separated by $2D$, while those corresponding to the XY transitions are separated by D. At $E \neq 0$, the inner lines corresponding to the X_2Y_2 and X_3Y_3 transitions are split into the lines corresponding to the X and Y components separated by an interval of $3E$, while the outer lines corresponding to the X_1Y_1 and X_4Y_4 transitions are split into the lines corresponding to the X and Y components separated by an interval of $9E$. First-order EPR spectra of septet molecules with $E = 0$ exhibit six lines corresponding to the single-photon XY and Z transitions, the lines corresponding to the Z_1 and Z_6 transitions being separated by an interval of $10D$.[1] At $E \neq 0$, the outer lines corresponding to the X_1Y_1 and X_6Y_6 transitions are split into the lines corresponding to the X and Y components with an interval of $15E$. In addition, in weak magnetic fields (< 100 mT) the EPR spectra of many quintet and septet molecules recorded in frozen organic solutions, argon matrices and polycrystals include signals corresponding to two-photon transitions ($\Delta m_s = 2$), and also extra signals from molecules with non-canonical orientations.[1] The first-order EPR spectra of high-spin molecules are observed only if the parameters D of these molecules are much less than the microwave quantum energy of the EPR spectrometer. For the X-band EPR spectrometers operating at ~ 9.5 GHz, the microwave quantum energy is about 0.33 cm^{-1}, being comparable with the D parameters of quintet and septet nitrenes. Therefore, the X-band EPR spectra of all quintet and septet nitrenes demonstrate complex patterns and show no symmetry relative to the point $g = 2$.

It was shown [50, 51] that the D_Q and E_Q parameters of the quintet dinitrenes composed of light atoms depend on the angle $\Theta = 2\alpha$ between the nitrene C – N bonds and on the

D_t parameters of the triplet centres in the quintet molecules, which are calculated from Eqn (3):

$$D_t = \frac{\rho_{NQ}}{\rho_{NT} D_T} \quad (3)$$

where D_T is the D parameter of triplet mononitrene (precursor of quintet dinitrene) experimentally determined from the EPR spectra, and ρ_{NQ} and ρ_{NT} are the quantum chemically calculated spin densities on the nitrene units in the quintet dinitrene and its triplet precursor, respectively. The dependences of D_Q and E_Q on α and D_t are described by Eqns (4) and (5)

$$D_Q = \frac{1}{6} D_t (3 \sin^2 \alpha - 1) \quad (4)$$

$$E_Q = \frac{1}{6} D_t (\cos^2 \alpha) \quad (5)$$

The plots of the magnitudes and signs of the D_Q and E_Q parameters of quintet dinitrenes *vs.* angle Θ and the orientations of the principal magnetic axes in their molecules are shown in Fig. 1.

The D_S and E_S parameters of the septet trinitrenes having C_{2v} symmetry and containing two equivalent nitrene centres with $D_{t1} = D_{t2} = D_t$ and the third nitrene centre with $D_{t3} = D_T (1 + \lambda)$, where

$$\lambda = \frac{D_{t3} - D_t}{D_t},$$

are described [52] by Eqns (6) and (7)

$$D_S = -\frac{D_t}{10} x \left(1 + \frac{\lambda}{3}\right) \quad (6)$$

$$E_S = \frac{D_t}{30} x \left[4 \cos^2\left(\frac{\theta}{2}\right) - 1 + \lambda\right] \quad (7)$$

Figure 2 presents the plots of the magnitudes and signs of the D_S and E_S parameters *vs.* angle Θ and the orientations of the principal magnetic axes in the molecules of these septet trinitrenes.

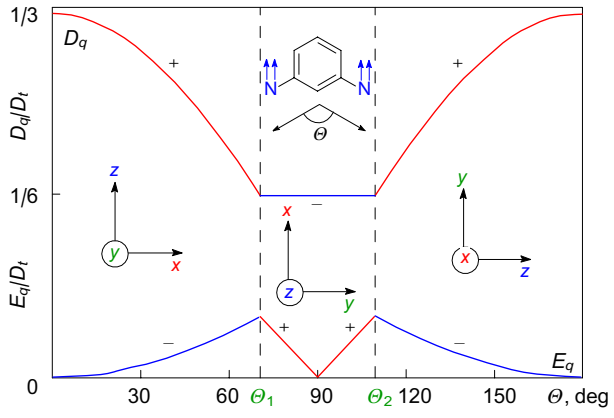


Figure 1. Zero-field splitting parameters D_Q and E_Q of quintet dinitrenes plotted *vs.* angle Θ using the data taken from Ref. 51. The orientations of the principal magnetic axes in the molecules of quintet dinitrenes are also shown.

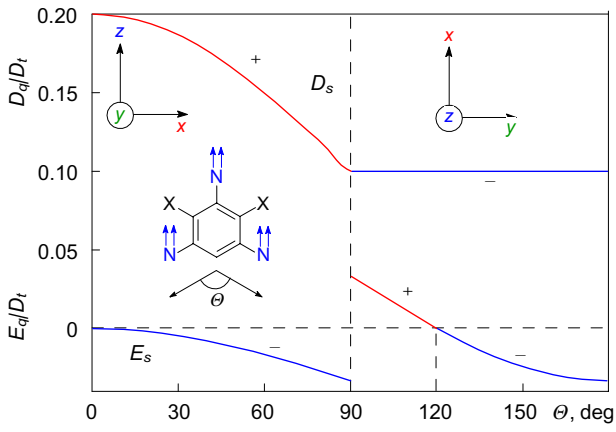


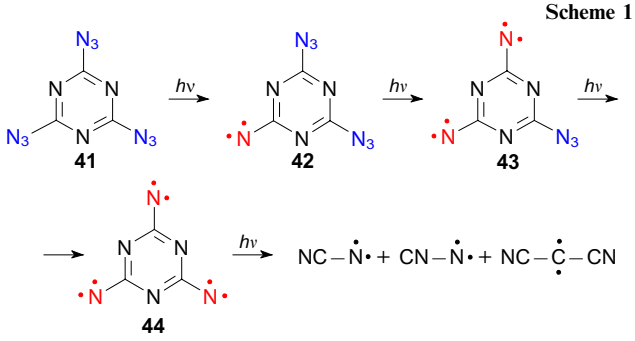
Figure 2. Zero-field splitting parameters D_S and E_S of septet trinitrenes with C_{2v} symmetry plotted *vs.* angle Θ using the data taken from Ref. 52. The orientations of the principal magnetic axes in the molecules of septet trinitrenes are also shown.

High-spin molecules possess magnetic properties at negative values of the parameters D, the height of the spin-inversion barrier separating the W_{-S} and W_{+S} states being proportional to D and to the squared spin S.[53–55] Quintet dinitrenes composed of light atoms are characterized by negative parameters D_Q and exhibit magnetic properties only in a narrow interval $70.6° < \Theta < 108.8°$ (see Fig. 1). Septet trinitrenes are characterized by negative parameters D_S at $\Theta > 90°$ (see Fig. 2). From Eqns (4) and (6), it also follows that the higher the spin densities on the nitrene centres of high-spin nitrenes the larger the D parameters; note that the spin density depends strongly on the nature of substituents in the aromatic nucleus. Heavy atoms located near the nitrene units in high-spin nitrenes have a particularly strong impact on the magnitudes and signs of the D parameters through the spin–orbit effects.[56, 57] Generally, the $\boldsymbol{D}$ tensor of high-spin molecules is the sum of two tensors, $\boldsymbol{D}^{SS}$ and $\boldsymbol{D}^{SOC}$, where $\boldsymbol{D}^{SS}$ is the dipole spin–spin interaction tensor and $\boldsymbol{D}^{SOC}$ is the spin–orbit coupling tensor characterizing the interaction between the unpaired electrons and excited electronic states.[55] For high-spin nitrenes consisting of light atoms the contribution $\boldsymbol{D}^{SOC}$ to the total tensor $\boldsymbol{D}$ is usually at most 10%;[58–60] however, it can be as large as 70% if the nitrene molecules contain heavy bromine atoms at distances of about 3 Å from the nitrene centres.[56]

4. High-spin nitrenes with *sym*-triazine skeleton

For long, triazide **41** was the one and only readily available precursor of high-spin nitrenes. Pioneering studies on the photolysis of single-crystalline triazide **41** at 113 K made it possible to detect the EPR signals of only triplet mononitrene **42** with $|D_T| = 1.44$ cm^{-1} and $|E_T| = 0.005$ cm^{-1} (Scheme 1).[61] This nitrene demonstrated a surprisingly high thermal stability, *viz.*, the intensities of the EPR signals remained unchanged for many days at room temperature. Three decades later, photolysis of single-crystalline triazide **41** was re-examined at 3.5 K.[62] Based on the EPR spectra obtained, it was shown that the reaction affords a quintet dinitrene **43** with $|D_Q| = 0.280$ cm^{-1} and $|E_Q| = 0.058$ cm^{-1} as the sole new product. The intensities of the EPR signals of dinitrene **43** demonstrated a Curie

Scheme 1



behaviour in the temperature range of 3.5–10 K and thus proved that the compound has a quintet ground spin state. The fact that septet trinitrene **44** was not detected among the reaction products was explained by inefficient photolysis of dinitrene **43** in the single crystal of triazide **41**.

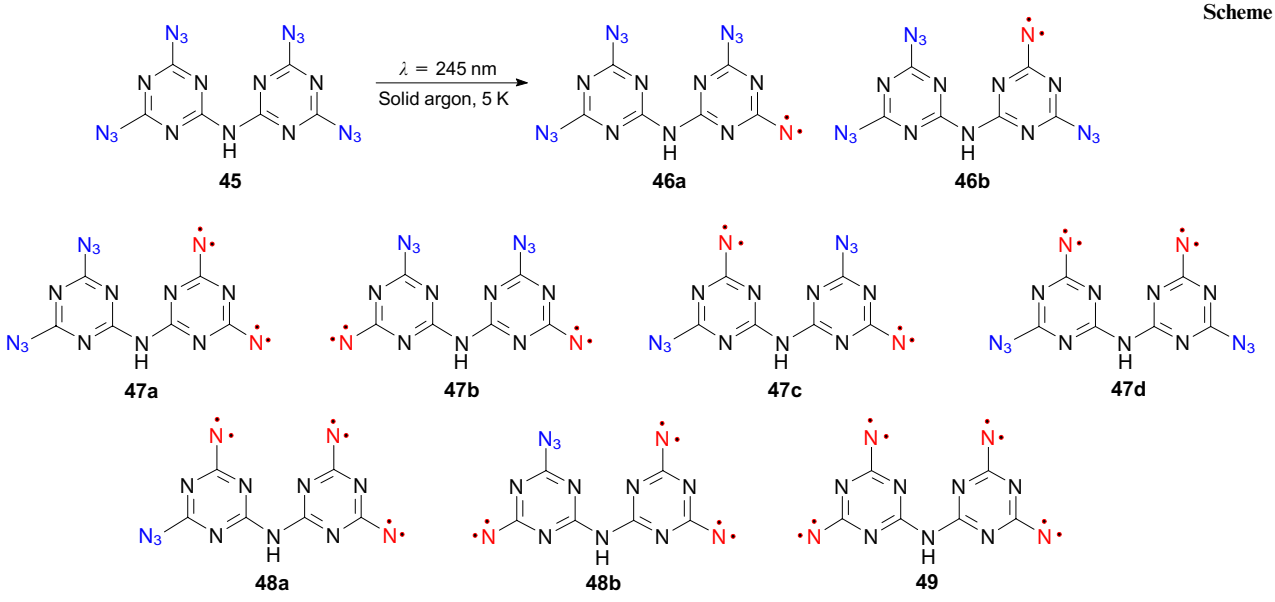
In 2004, photolysis of triazide **41** was again studied by UV, IR and EPR spectroscopies.[63,64] As applied to chemistry of septet nitrenes, experiments with solid inert-gas (nitrogen) matrices at 15 K were carried out for the first time. Irradiation of triazide **41** isolated in solid nitrogen by monochromatic light at $\lambda = 254$ nm caused successive formation of triplet nitrene **42**, quintet dinitrene **43** and septet trinitrene **44**; no side reactions were observed. Trinitrene **44** with $D_S = -0.123$ cm^{-1} and $E_S = 0$ was photochemically very unstable. The photodecomposition products of **44** included two triplet nitrenes, NCN and CNN, and one more triplet product which was later identified as triplet dicyanocarbene.[65] It was shown that high-spin nitrenes with *sym*-triazine skeleton bear very high spin densities on the nitrene centres and are characterized by the strongest spin–spin interactions on the biradical centres. However, the very low photochemical stability of trinitrene **44** may be a severe obstacle to practical applications of this system.

The possibility to generate high-spin nitrenes with *sym*-triazine skeleton and $S > 3$ was studied by EPR spectroscopy in relation to photolysis of tetraazide **45** in argon matrices at 5 K (Scheme 2).[66] According to quantum chemical calculations, nitrenes **46a**,**b**, **47a**–**d**, **48a**,**b** and **49** formed during the photolysis of compound **45** should have high-spin ground states that lie much lower than the excited low-spin states on the energy scale (Table 1). Quintet dinitrene **47b** with $\Theta = 103.5°$ should have a negative parameter D_Q in accordance with the diagram in Fig. 1 while septet trinitrene **48a** with $\Theta < 90°$ should be characterized by a positive D_S parameter in accordance with the diagram shown in Fig. 2.

Table 1. Energy gaps ΔE_{L-H} between the high-spin and low-spin states and the D and E parameters of nitrenes **46a**,**b**, **47a**–**d**, **48a**,**b** and **49** obtained from density functional theory B3LYP/TZVP calculations.[66]

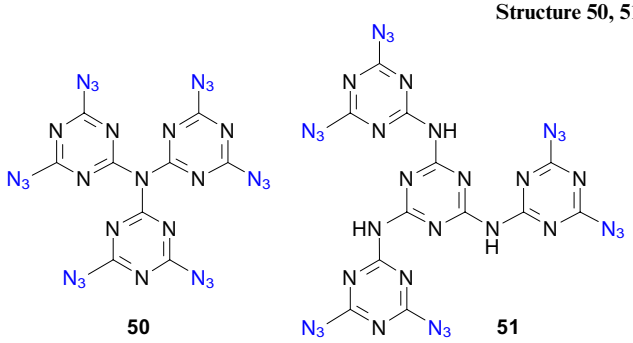
Nitrene	S	ΔE_{L-H}, kcal mol^{-1}	D, cm^{-1}	E, cm^{-1}
46a	1	0	+1.4555	0.0008
	0	37.0	–	–
46b	1	0	+1.4449	0.0017
	0	36.5	–	–
47a	2	0	+0.2845	0.0596
	1	30.2	–	–
	0	80.2	–	–
47b	2	0	−0.2469	0.0562
	1	10.6	–	–
	0	74.0	–	–
47c	2	0	+0.4094	0.0274
	1	10.6	–	–
	0	73.8	–	–
47d	2	0	+0.4700	0.0051
	1	10.5	–	–
	0	72.8	–	–
48a	3	0	+0.2114	0.0221
	2	9.9	–	–
	1	5.0	–	–
	0	112.0	–	–
48b	3	0	−0.1419	0.0339
	2	9.9	–	–
	1	66.4	–	–
	0	117.4	–	–
49	4	0	+0.1035	0.0290
	3	15.7	–	–
	2	31.5	–	–
	1	20.9	–	–
	0	151.0	–	–

Scheme 2



The experimental studies gave an unexpected result, *viz.*, it was found that photolysis of tetraazide **45** produces only two paramagnetic products, a triplet nitrene **46a** ($D_T = 1.45$ cm^{-1}, $E_T = 0.0045$ cm^{-1}) and a quintet dinitrene **47a** ($D_Q = 0.276$ cm^{-1}, $E_Q = 0.058$ cm^{-1}).[66] The low efficiency of photolysis of the azido groups in the second triazine ring of dinitrene **47a** was explained by fast intramolecular transfer of photoexcitation energy from the diazido-substituted triazine ring to the neighbouring dinitrenotriazide ring. By and large, photochemical studies of tetraazide **45** showed that generation of high-spin nitrenes with $S > 3$ from the polyazides **50** and **51** has no great prospects.

Structure 50, 51



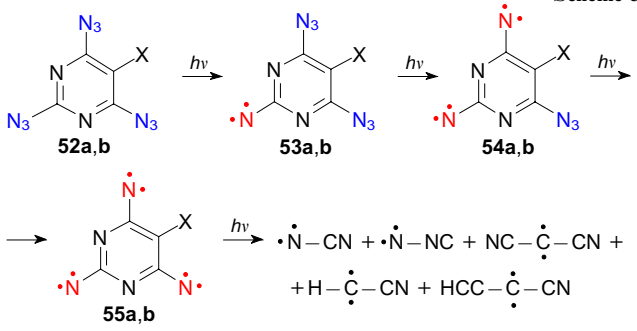
50 **51**

5. High-spin pyrimidinylnitrenes

To date, only two types of high-spin pyrimidinylnitrenes have been reported.[65] An EPR study revealed that photolysis of triazide **52a** and its chlorine-substituted derivative **52b** in argon matrices at 5 K is accompanied by successive formation of triplet nitrenes **53a**,**b**, quintet dinitrenes **54a**,**b** and septet trinitrenes **55a**,**b** (Scheme 3). The magnetic parameters of all these nitrenes are listed in Table 2.

Compared to septet trinitrene **44**, the septet trinitrenes **55a**,**b** are characterized by smaller D_S parameters (by about 9% in absolute value) and weaker magnetic properties. This is due to more efficient spin density delocalization from the nitrene centres in the aromatic nucleus containing the smaller number of endocyclic nitrogen atoms and the larger total number of atoms in the molecules.[65] Similarly to trinitrene **44**, compounds **55a**,**b** appeared to be photochemically unstable. Photodecomposition of trinitrene **55a** under irradiation at $\lambda = 254$ nm results in the formation of triplet nitrenes NCN and CNN and triplet carbenes NCCCN, HCCN and HCCCCN. The last-mentioned carbene was never generated before under laboratory conditions; however, it was spectroscopically detected[67] in the circumstellar envelope of star IRC+10216 a few years before the studies of trinitrene **55a**. Photodecomposition of trinitrene **55b** results in two paramagnetic products, namely, triplet nitrenes NCN and CNN.

Scheme 3



X = H (**a**), Cl (**b**)

Table 2. Parameters D and E of nitrenes **53a**,**b**, **54a**,**b** and **55a**,**b**.[65]

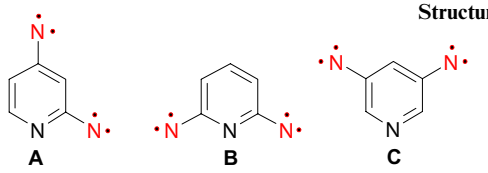
Nitrene	S	D, cm^{-1}	E, cm^{-1}
53a	1	1.260	0.0046
53b	1	1.170	0.0044
54a	2	0.241	0.0540
54b	2	0.231	0.0540
55a	3	−0.1122	−0.0035
55b	3	−0.1119	−0.0058

6. High-spin pyridylnitrenes

6.1. Quintet pyridyldinitrenes

There are three possible types of quintet pyridyldinitrenes (see structures **A**, **B** and **C**). At present, the magnetic parameters of the type **A** and type **B** dinitrenes have been determined.

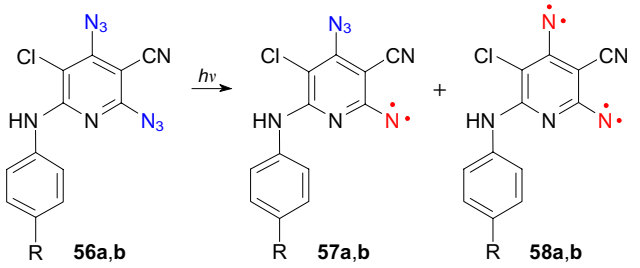
Structures A–C



A **B** **C**

EPR spectroscopy studies revealed that photolysis of diazides **56a**,**b** in frozen solutions of 2-methyltetrahydrofuran (MTHF) at 77 K proceeds selectively and affords mixtures of triplet nitrenes **57a**,**b** and quintet dinitrenes **58a**,**b** (Scheme 4).[68,69]

Scheme 4



56a,**b** **57a**,**b** **58a**,**b**

R = Me (**a**), Br (**b**)

The magnetic parameters D_Q and E_Q of dinitrenes **58a**,**b** are close to those of dinitrenes **1** and **35**. All these systems have very similar EPR spectra characteristic of the quintet dinitrenes with $\Theta \approx 120°$ and $|E_Q/D_Q| \approx 1/5$. As in the case of photolysis of triazides **52a**,**b**, the azido groups adjacent to endocyclic nitrogen atoms are more photolabile in the photolysis of diazides **56a**,**b**.

Photolysis of diazides **59a**,**b** in frozen MTHF solutions at 77 K also produces mixtures of triplet nitrenes **60a**,**b** and quintet dinitrenes **61a**,**b** (Scheme 5).[50,51,70–72] In contrast to the EPR spectra of dinitrenes **1**, **35** and **58a**,**b**, those of

Scheme 5

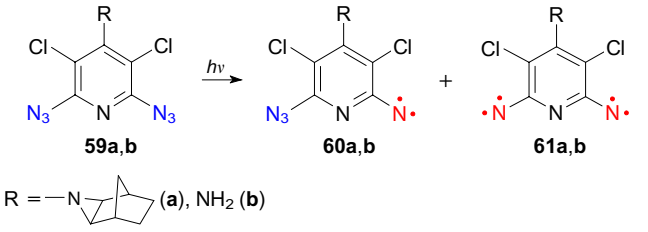


Table 3. Parameters D_Q and E_Q of dinitrenes **58a**,**b** and **61a**,**b** (argon matrix, 5 K).

Nitrene	Matrix	$\|D_Q\|$, cm^{-1}	$\|E_Q\|$, cm^{-1}	Ref.
58a	MTHF	0.211	0.043	69
58b	MTHF	0.219	0.044	69
61a	MTHF	0.191	0.0625	50
61b	MTHF	0.202	0.0664	50
61b	Argon	0.210	0.056	51

dinitrenes **61a**,**b** obey a pattern characteristic of the quintet molecules with abnormally large E_Q values (Table 3).

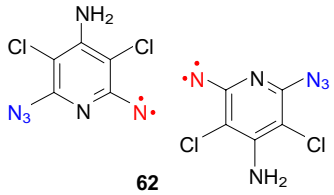
Equations (4) and (5) relating the angles Θ to the D_Q and E_Q parameters of quintet dinitrenes were for the first time used in the studies of dinitrenes **61a**,**b**.[50] From these equations it followed that the molecules of dinitrenes **61a**,**b** with $\Theta \approx 114.5^\circ$ should be characterized by a $|E_Q/D_Q|$ ratio of about 1/4. Large values of the E_Q parameters of dinitrenes **61a**,**b** in the MTHF solutions were explained by the formation of molecular complexes between these dinitrenes and MTHF molecules.[71] Indeed, more recent studies of the EPR spectra of dinitrene **61b** in argon matrices confirmed that the E_Q parameter of this dinitrene is much smaller (see Table 3) provided that no complexation occurs.[51,72] The most important result of these investigations was the construction of the diagram (see Fig. 1) describing the dependence of the magnitudes and signs of the parameters D_Q and E_Q, as well as the orientations of the principal magnetic axes in the molecules of quintet dinitrenes on the angle Θ.[51]

The formation of molecular complexes between triplet and quintet nitrenes and MTHF molecules manifests itself as intense colouration of the frozen solutions of diazides **56a**,**b** and **59a**,**b** under UV irradiation. For instance, short-term (30 s) irradiation of diazide **59b** in MTHF glass at 77 K by light with $\lambda = 245$ nm caused the appearance of strong UV absorption bands with maxima at 356, 492 and 524 nm and the sample turned purple.[73] On further UV irradiation, two strong absorption bands with maxima at 375 and 638 nm appeared in the UV spectrum and the colour of the sample changed to blue-green. According to quantum chemical calculations, none of the UV spectra described above can be assigned to nitrenes **60b** and **61b**; most probably, they correspond to complexes of these nitrenes with the MTHF molecules.[74]

Based on the IR spectral data, it was established that many pyridylnitrenes readily enter into reactions of nitrene insertion into the pyridine ring resulting in diamagnetic diazacycloheptatetraenes, which are undetectable by EPR spectroscopy.[75] Such processes are highly undesirable for target generation of high-spin nitrenes. Meanwhile, IR spectroscopy studies also showed that photolysis of diazide **59a** in argon matrices (17 h of irradiation at $\lambda > 350$ nm) yields only two products, *viz.*, nitrenes **60a** and **61a** in a 1 : 2 ratio.[76] High photochemical stability of these nitrenes was explained by the presence of chlorine atoms at β-positions of the pyridine ring, which efficiently protect the pyridine ring from being attacked by the nitrene centres.

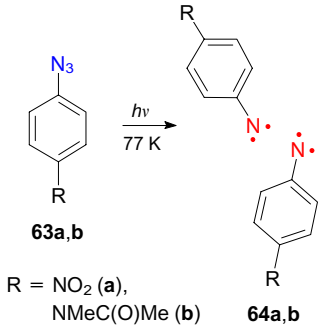
To date, only one bimolecular quintet dinitrene generated during the photolysis of crystalline aryl diazides has been characterized. This is dimer **62** ($D_Q = 0.251$ cm^{-1}, $E_Q = 0.030$ cm^{-1}) produced by photolysis of polycrystalline diazide **59b** at 77 K.[77]

Structure 62



It is stable only at cryogenic temperatures. The D_Q and E_Q parameters of dimer **62** correspond to a bimolecular structure with the angle Θ between the nitrene C—N bonds equal to about 133°. X-Ray diffraction data confirmed that the C—N_3 bonds in adjacent molecules in the crystal lattice of the parent diazide **59b** are arranged at just this angle.[77] Prior to the generation of dimer **62**, the formation of bimolecular quintet dinitrenes was observed only during the photolysis of crystalline phenyl azides **63a**,**b** (Scheme 6).[78] According to X-ray diffraction data, the angles Θ between the nitrene C—N bonds in dimers **64a**,**b** are nearly 165° while the dimers were approximately characterized by the parameters $D_Q = 0.328$ cm^{-1} and $E_Q = 0.0003$ cm^{-1}. From the temperature dependence of the EPR signal intensities it follows that the quintet states of dimers **64a**,**b** are excited ones and lie ~80 cal mol^{-1} higher than the triplet states on the energy scale. Mention was made that bimolecular quintet dinitrenes are formed only if $\Theta < 180^\circ$ and the distances between the nitrene nitrogen atoms exceed 3.6 Å. Such a specific arrangement of molecules in the crystals of the parent phenyl azides is favoured by the presence of highly polar substituents (*para*-nitro and *para*-*N*-methylacetamide groups) in the phenyl ring. Quintet dimers **64a**,**b** appeared to be thermally unstable and completely disappeared on heating the crystals to 100 K.

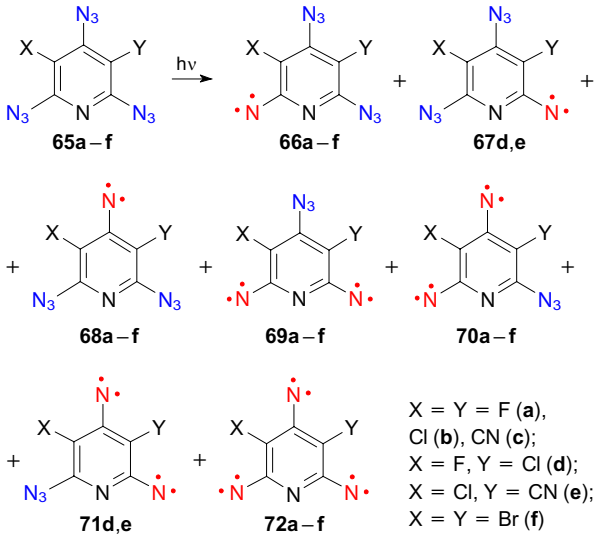
Scheme 6



6.2. Septet pyridyltrinitrenes

To date, the magnetic parameters were determined for six septet pyridyltrinitrenes **72a**–**f** generated during the photolysis of triazides **65a**–**f** in argon matrices at 5–13 K (Scheme 7).[52,79–83] According to EPR spectroscopy data, the yield of trinitrenes **72b**–**f** is at most 6%.[52,80–83] Pho-

Scheme 7



tolysis of triazides **65b–f** produces isomeric triplet nitrenes **66b–f**, **67d,e** and **68b–f** as major products with a total yield of 50%–55%. The only exception is trinitrene **72a**, the sole product of photolysis of triazide **65a** (according to IR spectroscopy data), which is formed in nearly quantitative yield.[84] This trinitrene is the first septet system whose ideal experimental IR spectrum is available. Moreover, based on the IR spectra it was established that photolysis of triazide **65a** proceeds selectively and begins with the formation of only two compounds, triplet nitrene **66a** and quintet dinitrene **69a**. A similar selectivity was observed in the study of photolysis of triazide **65b** in MTHF glasses at 77 K.[85] Selective photodecomposition of azido groups in α-positions of pyridine ring was also observed during the photolysis of triazides **65c–f** in argon matrices.[81–83] All these data are in good agreement with selective photolysis of α-azido groups in diazides **56a,b** (see Scheme 4).[68]

Triplet nitrenes **66a,c** bearing lower spin densities on nitrene centres are characterized by $D_T = 1.02–1.08$ cm^{-1} and $E_T = 0$, whereas isomeric triplet nitrenes **68a,c** are characterized by $D_T = 1.14–1.16$ cm^{-1} and $E_T = 0$.[52,81–83] Nitrenes **66b,e**, **67e** and **68b,d,e** containing chlorine atoms in *ortho*-positions relative to the nitrene centres have no cylindrical symmetry and are characterized by $E_T = 0.0018–0.0035$ cm^{-1} (Refs 52, 82, 83). The magnetic parameters of quintet dinitrenes **70a–e** and **71d,e** are very close in absolute value to the D_Q and E_Q parameters of quintet dinitrenes **58a,b** (see Table 3). The magnetic parameters of structurally similar quintet dinitrenes **61a,b** and **69a–e** are also close. Compared to septet trinitrenes **44** and **55a,b**, the septet pyridyltrinitrenes **72a–e** have lower spin densities on nitrene centres and, as a consequence, have smaller (in absolute value) parameters D_S (Table 4). A study of septet trinitrene **72b** made it possible to derive Eqns (6) and (7) and to construct the diagram (see Fig. 2) describing the dependence of the magnitudes and signs of the parameters D_S and E_S, and the orientations of the principal magnetic axes in the molecules of septet trinitrenes (C_{2v} symmetry) on the angle Θ.[52]

Nitrenes generated during the photolysis of dibromo-substituted triazide **65f** represent a particular case.[81] Triplet nitrene **66f** with $D_T = 1.285$ cm^{-1} and $E_T = 0.005$ cm^{-1} is the major reaction product (yield is about 40%).[81] In addition, the reaction affords quintet dinitrenes **69f** (~30%) and **70f** (~24%) and a septet trinitrene **72f** (~6%) with extraordinary high parameter D_S. Quantum chemical calculations showed that the D parameters of nitrenes **69f**, **70f** and **72f** are abnormally high owing to the presence of heavy bromine atoms in these molecules since the Br atoms considerably increase the contribution of spin–orbit coupling to the total parameters D^{Tot} (Table 5). For trinitrene **72f**, D^{SOC} is almost twice as high as D^{SS} and determines the sign of the parameter D^{Tot}. A clear manifestation of the 'heavy-atom effect', as applied to magnetic anisotropy of septet pyridyltrinitrenes, is demonstrated in Fig. 3. It should be noted that the heavy-atom effect on the parameters D^{Tot} of high-spin nitrenes manifests itself only if the distance between the nitrene centres and heavy atoms is at most 3.09 Å.[56] At longer distances, the heavy-atom effect rapidly decreases (Fig. 4).

In the molecule of dinitrene **69f**, the nitrene units are more distant from bromine atoms and the D^{SS} and D^{SOC} contributions to the total parameter D^{Tot} are nearly equal. A fundamentally different picture is observed for dinitrene **70f** with shorter distances between the nitrene centre at position 4 of pyridine ring and two bromine atoms, *viz.*, the D^{SOC} contribution is about 1.5 times larger than D^{SS}.

Table 4. Parameters D_S and E_S of septet trinitrenes **72a–e**.

Nitrene	D_S, cm^{-1}	E_S, cm^{-1}	Ref.
72a	−0.1018	0.0037	79
72b	−0.1019	0.0033	52
72c	−0.1011	0.0043	80
72d	−0.1017	0.0042	82
72e	−0.1021	0.0034	83

Table 5. Experimental and calculated ZFS parameters (in cm^{-1}) of nitrenes **69f**, **70f** and **72f**.[81]

Nitrene	S	D^{SS}	D^{SOC}	D^{Tot}	$(E/D)^{Tot}$	D^{Exp}	$(E/D)^{Exp}$
69f	2	0.187	0.186	0.373	0.16	0.289	0.198
70f	2	0.210	0.344	0.367	0.16	0.373	0.169
72f	3	−0.101	0.213	0.249	0.10	0.297	0.060

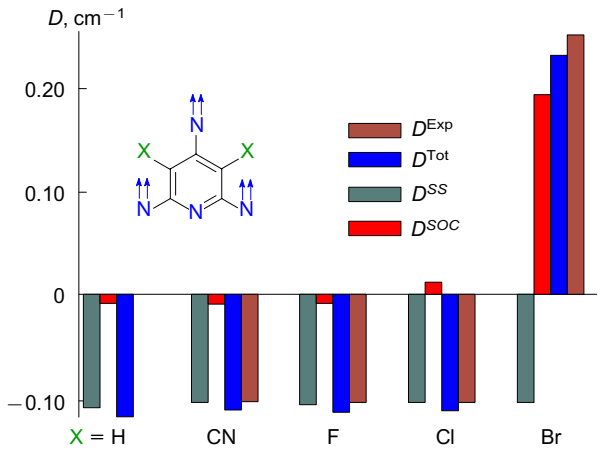


Figure 3. Parameters D^{SS}, D^{SOC}, D^{Tot} and D^{Exp} of different septet pyridyltrinitrenes. The plot is based on the data taken from Ref. 86.

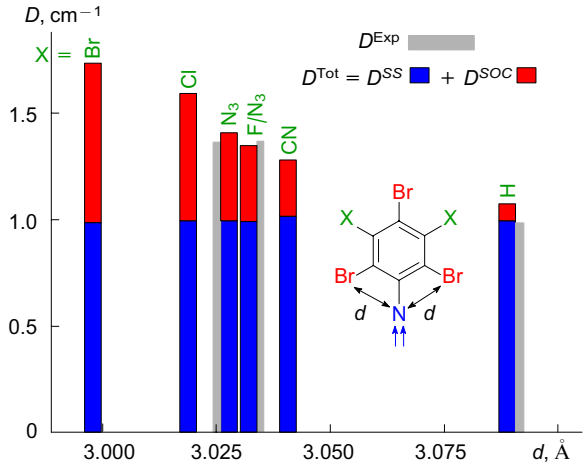
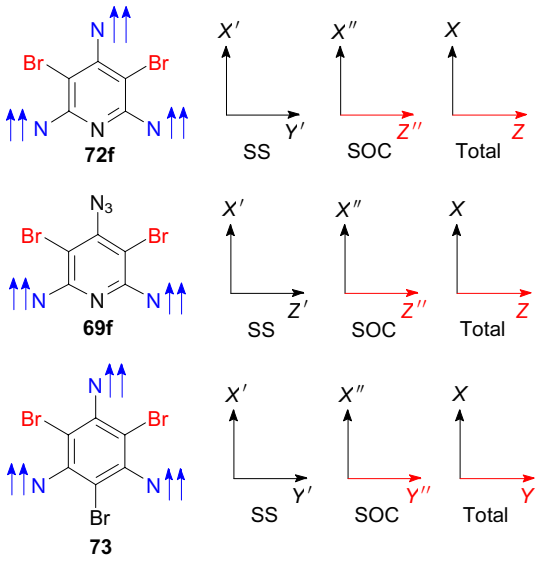


Figure 4. Parameters D^{SS}, D^{SOC} and D^{Exp} of certain triplet phenylnitrenes. The plot is based on the data taken from Ref. 56.

The study of nitrenes **69f**, **70f** and **72f** for the first time demonstrated that, in principle, the magnetic anisotropy of high-spin molecules can be considerably increased by introducing heavy atoms. However, it was found that trinitrenes containing two heavy atoms in the pyridine ring have easy-plane type magnetic anisotropy and exhibit no dynamic magnetic properties (see Fig. 3) owing to different orientation of the principal magnetic axes Z' and Z'' of the $\boldsymbol{D}^{SS}$ and $\boldsymbol{D}^{SOC}$ tensors. According to quantum chemical calculations of trinitrene **72f**, the Z'' axis of the $\boldsymbol{D}^{SOC}$ tensor lies in the plane of the pyridine ring and is directed along the line connecting two bromine atoms, whereas the Z' axis of the $\boldsymbol{D}^{SS}$ tensor is perpendicular to that plane.[81] Therefore, diagonalization of the $\boldsymbol{D}^{Tot}$ tensor for $D^{SS} = -0.101$ cm^{-1} and $D^{SOC} = 0.213$ cm^{-1} gives $D^{Tot} = 0.036(SS) + 0.213(SOC) = 0.249$ cm^{-1}, which is in good agreement with the experiment. In the molecule of trinitrene **72f**, the Z axis of the $\boldsymbol{D}^{Tot}$ tensor is aligned with the Z'' axis of the $\boldsymbol{D}^{SOC}$ tensor (main component of the internal magnetic anisotropy). In addition, calculations predict a large negative parameter $D^{Tot} = -0.242$ cm^{-1} for tribromo-substituted septet trinitrene **73** with the same orientation of the Z' and Z'' axes of the $\boldsymbol{D}^{SS}$ and $\boldsymbol{D}^{SOC}$, tensors, respectively, owing to high symmetry (D_{3h}) of this molecule.[81] Parallel orientations of the Z' and Z'' axes of the $\boldsymbol{D}^{SS}$ and $\boldsymbol{D}^{SOC}$ tensors were also observed for the molecule of dinitrene **69f** due to the same spatial orientation of nitrene centres and bromine atoms. Therefore, the D^{Tot} parameter of dinitrene **69f** is the scalar sum of D^{SS} and D^{SOC} (see Table 5).

Structures 69f, 72f, 73



Magnetization measurements using a SQUID magnetometer showed that UV irradiation of crystalline triazide **65b** at $\lambda = 200-400$ nm for 30 min at 2 K causes the sample to undergo a transition from diamagnetic to paramagnetic state with the maximum magnetization corresponding to nearly $S = 2$ effective spin state and thus to confirm the possibility to design, in principle, magnetic materials based on high-spin nitrenes.[87] An independent EPR spectroscopy study revealed that photolysis of crystalline triazides **65b** and **65c** at 77 K yields quintet dinitrenes **69b**,**c** and **70b**,**c** in a 4:1 ratio as major products.[88] Unfortunately, the total quantum yield of dinitrenes was as low as 0.0004 due to the loss of the crystals transparency in the early stages of photolysis. γ-Radiolysis of crystals of triazides **65b** and **65c** at 77 K appeared to be more efficient, namely, the total yield of dinitrenes **69b**,**c** and **70b**,**c** increased 30-fold upon irradiation with a dose of 1000 kGy.[88–93] The dinitrenes **69b**,**c** and **70b**,**c** formed in a 6:1 ratio, demonstrated a rather high thermal stability in crystals of the parent triazides, while their signals in the EPR spectra completely disappeared only at $T > 235$ K.

The only attempt to detect UV spectra of septet pyridyltrinitrenes in organic glasses was reported.[73] It was found that photolysis of triazide **65b** in MTHF solutions frozen at 77 K causes successive generation of triplet nitrene **66b**, quintet dinitrene **69b** and septet trinitrene **72b**. The UV spectrum of each nitrene exhibited strong absorption bands with maxima at 499 and 527 nm for nitrene **66b**, at 576 and 620 nm for dinitrene **69b** and at 709 nm for trinitrene **72b**. According to EPR spectroscopy data, septet trinitrene **72b** isolated in frozen MTHF solutions at 77 K is characterized by $|D_S| = 0.100$ cm^{-1} and $|E_S| = 0.0005$ cm^{-1} (Ref. 46). These magnetic parameters are significantly different from those of this trinitrene in solid argon (see Table 4). The differences in the magnetic parameters of trinitrene **72b** can be explained by its complexation with MTHF; therefore, the UV spectra of nitrenes **66b**, **69b** and **72b** recorded in MTHF glasses should be assigned to the molecular complexes of these nitrenes with solvent molecules.

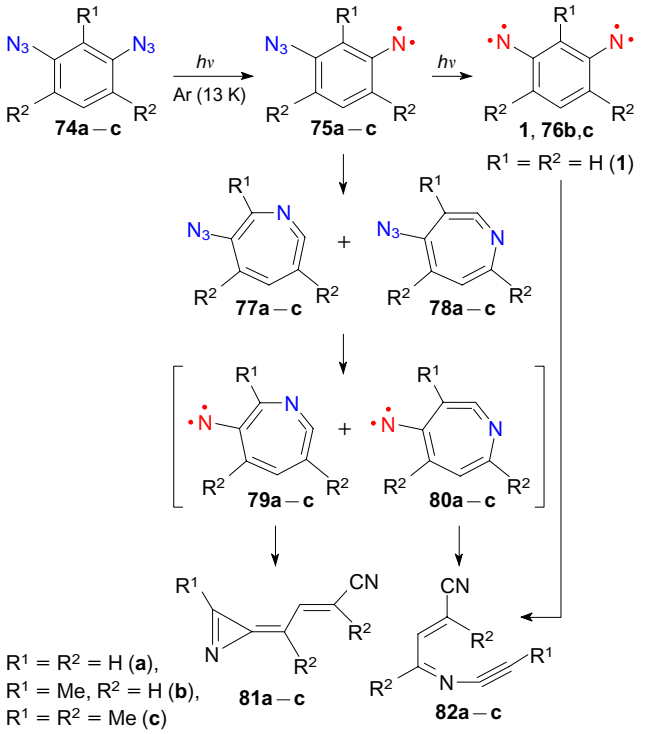
7. High-spin nitrenobenzenes

7.1. Quintet *m*-phenylenedinitrenes

The yield of quintet dinitrene **1** generated during the photolysis of diazide **74a** and accompanying side reactions remained unknown until 2003. To clarify these issues, photolysis of diazides **74a–c** in solid argon matrices at 13 K was studied by IR and UV spectroscopies (Scheme 8).[94] Paramagnetic products of photolysis of diazides **74a–c** in MTHF glasses at 77 K were also studied by EPR spectroscopy.

Irradiation of diazide **74a** in argon matrices at $\lambda > 300$ nm produced a variety of paramagnetic and diamagnetic products.[94] The maximum yield of quintet dinitrene **1** (34%) was observed after 1 min of irradiation. Other products generated in this stage of photolysis included triplet nitrene **75a** (45%) and azacycloheptatetraenes **77a** (7%) and **78a** (14%). Compounds **77a** and **78a** are formed

Scheme 8

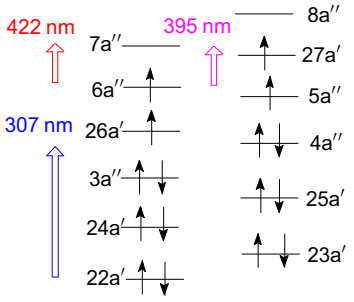


as a result of insertion of the nitrene centre into the benzene ring of nitrene **75a**. Signals of quintet dinitrene **1** completely disappeared in the IR spectra after 90 s of irradiation and the reaction resulted in diamagnetic compounds **81a** and **82a** as final products.

Photolysis of diazide **74b** was accompanied by generation of a mixture of triplet nitrene **75b** (44%), quintet dinitrene **76b** (maximum yield was 44% after 2 min of UV irradiation) and diamagnetic compound **78b** (12%).[94] Owing to the presence of protective methyl group in the benzene ring, the attack of the nitrene centre on the methylated carbon atom in nitrene **75b** was completely blocked. Further UV irradiation led to disappearance of the signals of nitrenes **75b** and compound **76b** in the IR spectra and to the appearance of corresponding signals of conformational isomers of compound **82b**, which are formed in a total yield of more than 90%. Ultraviolet spectroscopy studies showed that triplet nitrene **75b** isolated in argon matrices is characterized by the absorption bands with maxima at 309, 324, 401, 408, 418, 422 and 434 nm, while quintet dinitrene **76b** formed from compound **75b** is characterized by the absorption bands with maxima at 307, 326, 395, 418 and 422 nm. An analysis of the UV-Vis spectrum of dinitrene **76b** carried out within the framework of multiconfigurational quasi-degenerate second-order perturbation theory (MCQDPT2) showed that the absorption bands with maxima at 307, 326, 395, 418 and 422 nm correspond to different π → SOMO- and SOMO → π* transitions, *e.g.*, 22a′ → 26a′, 5a″ → 7a″ and 6a″ → 7a″ (Scheme 9).[74] Similar π → SOMO- and SOMO → π* transitions also occur in the case of triplet phenylnitrenes.[95,96] By and large, the electronic absorption spectra of triplet and quintet nitrenes have very much in common with those of benzyl ($PhCH_2^{\bullet}$) and aniline ($PhNH^{\bullet}$) radicals.[95]

Diazide **74c** with non-coplanar arrangement of azido groups was the least sensitive to UV irradiation. Indeed,

Scheme 9



photolysis of **74c** at $\lambda > 300$ nm for 30 min gave a quintet dinitrene **76c** as the sole product that demonstrated a high photochemical stability and decomposed to compounds **81c** and **82c** only after 9 h of irradiation at $\lambda > 300$ nm.[94]

An EPR study of products of the photolysis of diazides **74a–c** in MTHF solutions frozen at 77 K allowed one to detect very weak signals corresponding to the Z_4-transitions of quintet dinitrenes **1** and **76b**,**c**; these signals were used to determine the ZFS parameters of quintet *m*-phenylenedinitrenes with high accuracy for the first time.[94] More recently, the numerical values of the parameters D_Q and E_Q of dinitrenes **1** and **76b**,**c** were refined using modern line-shape EPR spectral simulations (Table 6).[97,98] Small differences between the experimental D_Q and E_Q values for dinitrene **1** (see Table 6) seem to be due to slightly different conditions for generation of this dinitrene (concentrations of solutions, UV radiation wavelengths, and duration of photolysis). Since methylated dinitrenes **76b**,**c** bear lower spin densities on nitrene centres and are characterized by large angles Θ, their parameters D_Q and E_Q are smaller than those of dinitrene **1** in excellent agreement with Eqns (4) and (5).

Table 6. Parameters D_Q and E_Q of dinitrenes **1**, **4–6** and **76b**,**c** (MTHF, 77 K).

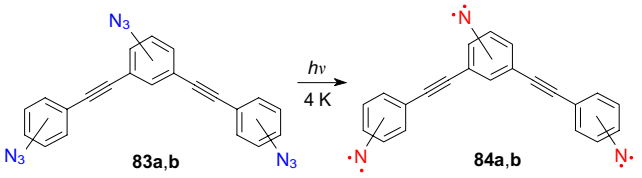
Nitrene	$\lvert D_Q\rvert$, cm^{-1}	$\lvert E_Q\rvert$, cm^{-1}	Ref.
1	0.202	0.040	97
1	0.205	0.041	98
76b	0.198	0.034	97
76c	0.184	0.035	97
4	0.223	0.034	98
5	0.202	0.041	98
6	0.187	0.038	98

The magnetic parameters of previously described quintet dinitrenes **4–6** ($D_Q \approx 0.15$ cm^{-1} and $E_Q \approx 0.002$ cm^{-1})[36,37] were recently refined using modern line-shape EPR spectral simulations.[98] It was proved that the D_Q and E_Q values of these dinitrenes are much larger (see Table 6).

7.2. High-spin oligoarylnitrenes

Oligo- and polyaromatic compounds can be used to synthesize aromatic oligo- and polyazides that can be photolyzed to generate high-spin nitrenes with $S > 3$. For instance, magnetization measurements showed that photolysis of polycrystalline triazides **83a**,**b** at 4 K gives paramagnetic products with $S = 2.9$, which correspond to septet trinitrenes **84a**,**b** (Scheme 10).[99] However, photolysis of polycrystalline pentaazide **85** produced a paramagnetic product

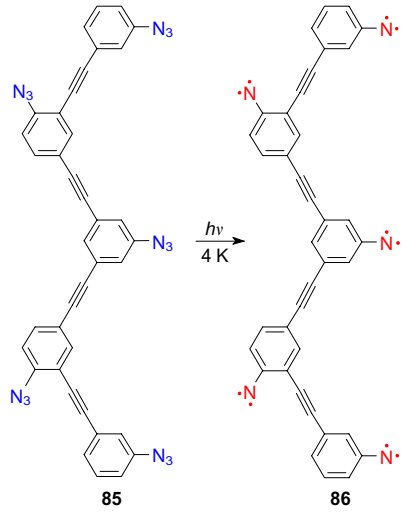
Scheme 10



a: 4-N_3/N, 3′-N_3/N, 4″-N_3/N; **b**: 3-N_3/N, 4′-N_3/N, 3″-N_3/N

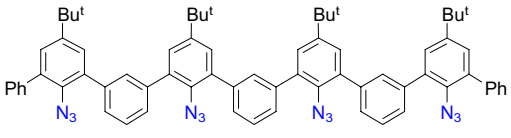
with an effective spin S of nearly 3, which indicated a non-quantitative yield of undecet pentanitrene **86** (Scheme 11). Unfortunately, the EPR spectra of the products of photolysis of triazides **83a**,**b** and pentaazide **85** in MTHF at 77 K appeared to be too complicated for being used to obtain even rough estimates of the magnetic parameters of the high-spin nitrenes.

Scheme 11



An attempt to generate a nonet tetranitrene by photolysis of tetraazide **87** in MTHF at 77 K showed that the paramagnetic products include a triplet nitrene ($D_T = 0.934$ cm^{-1}, $E_T = 0$ cm^{-1}) and two unidentified quintet dinitrenes with parameters $D_Q = 0.323$ cm^{-1}, $E_Q = 0.016$ cm^{-1} and $D_Q = 0.340$ cm^{-1}, $E_Q = 0.011$ cm^{-1}.[100, 101] The main products of the reactions were isomeric carbazoles (42% total yield) formed due to interactions of the nitrene units with the adjacent phenyl substituents. The absence of the nonet and septet products in the photolysis of tetraazide **87** was explained by the occurrence of side reactions.

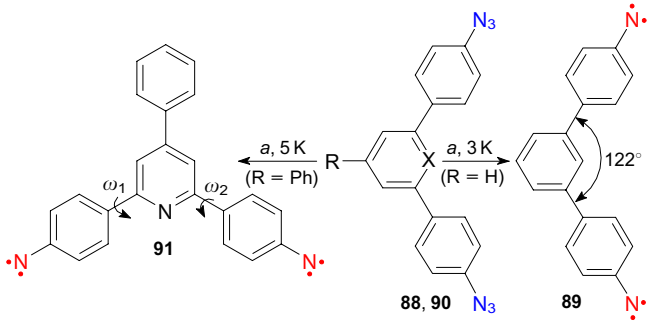
Structure 87



87

The determination of the magnetic parameters of high-spin oligoarylnitrenes from their EPR spectra is a complicated task.[102, 103] It was reported that photolysis of diazide **88** in MTHF at 3 K affords triplet nitrene **89** ($D_T = 0.929$ cm^{-1}, $E_T = 0$ cm^{-1}) and quintet dinitrene **91** with $D_Q = 0.2009$ cm^{-1} and $E_Q = 0.0358$ cm^{-1} (Scheme 12).[102]

Scheme 12



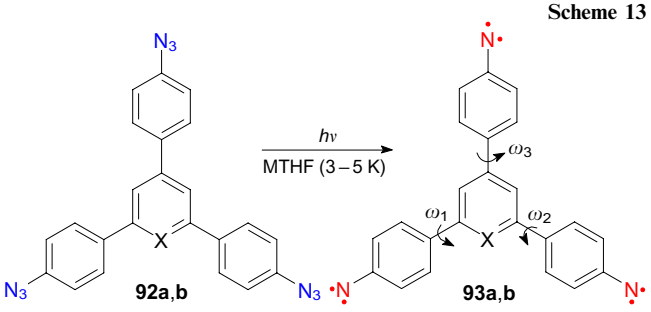
(*a*) *hν*, MTHF; R = H, X = CH (**88**); R = Ph, X = N (**90**)

However, according to Eqn (4) dinitrene **89** with $\Theta = 122°$ should show $D_Q \leqslant 0.186$ cm^{-1}. Presumably, the D_Q value of dinitrene **89** is overestimated when the existence of numerous rotational conformers of this dinitrene with different angles of rotation, ω_1 and ω_2, of the phenylnitrene moieties relative to the plane of the central aromatic ring is ignored. In fact, the experimental EPR spectrum of such a system represents a superposition of the EPR spectra of many individual conformers of dinitrene **89** with significantly different parameters D_Q and E_Q.[103] Therefore, the computer simulations of the EPR spectra of such conformers requires the use of not only conventional parameters (g, D and E) of the spin Hamiltonian, but also rather large line broadening parameters $\Gamma(D)$ and $\Gamma(E)$.

Exact determination of the magnetic parameters of conformationally flexible high-spin oligoarylnitrenes from their EPR spectra was for the first time performed in a study of quintet dinitrene **91** formed during the photolysis of diazide **90** in MTHF at 5 K (see Scheme 12).[103] The results obtained for dinitrene **91** are as follows: $g = 2.003$, $D_Q = 0.154$ cm^{-1} and $E_Q = 0.050$ cm^{-1}, being characteristic of quintet dinitrenes with $\Theta \approx 112°$. Computer simulations of the experimental EPR spectrum of dinitrene **91** was done using the parameter $\Gamma(E_Q) = 1200$ MHz (0.04 cm^{-1}), which takes into account the presence of many conformers with twist angles ω_1 and ω_2 varied from $-9°$ to $-63°$. For such twist angles ω_1 and ω_2, the angle Θ was 111.2–114.6°, while the parameters D_Q and E_Q were varied in the ranges of 0.013 and 0.005 cm^{-1}, respectively. The most stable conformer of dinitrene **91** is characterized by the angles $\omega_1 = -19.8°$, $\omega_2 = +19.8°$, $\Theta = 111.8°$ and quantum chemical calculations predict $g = 2.0036$, $D_Q = 0.1709$ cm^{-1} and $E_Q = 0.0505$ cm^{-1} for this system.

According to the published data, photolysis of triazide **92a** in MTHF at 3 K causes the formation of triplet nitrene ($D_T = 0.9312$ cm^{-1}, $E_T = 0$ cm^{-1}), three isomeric quintet dinitrenes ($D_Q = 0.2123$ cm^{-1}, $E_Q = 0.0326$ cm^{-1}, $D_Q = 0.1942$ cm^{-1}, $E_Q = 0.0385$ cm^{-1} and $D_Q = 0.1751$ cm^{-1}, $E_Q = 0.0448$ cm^{-1}) and a septet trinitrene **93a** ($D_S = -0.0912$ cm^{-1}, $E_S = -0.0039$ cm^{-1}), as shown in Scheme 13.[102] The generation of three different quintet dinitrenes from symmetric triazide **92a** is hard to explain. Probably, the use of simulated EPR spectra of these three dinitrenes was necessary for better reproduction of the experimental EPR spectrum when calculations ignore the parameter $\Gamma(E)$. For instance, a more recent [104] simulation of the experimental EPR spectrum of the products of photolysis of triazide **92b** in MTHF at 5 K using the parameters $\Gamma(E)$ made it possible to identify the production

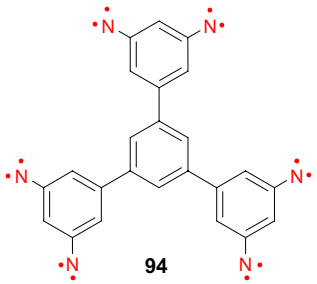
Scheme 13



of only three nitrenes, *viz.*, a triplet nitrene with $D_T = 0.920$ cm^{-1}, $E_T = 0$, a quintet dinitrene with $D_Q = 0.204$ cm^{-1}, $E_Q = 0.035$ cm^{-1} and a septet trinitrene **93b** with $D_S = -0.0904$ cm^{-1}, $E_S = -0.0102$ cm^{-1} (see Scheme 13). Based on these data, it was established that the first stage of photolysis of triazide **92b** involves selective decomposition of the azido group in the γ-azidophenyl moiety. After 45 min of irradiation the signal of triplet mononitrene in the EPR spectra completely disappeared and the yield of trinitrene **93b** was as high as nearly 70%.

The EPR spectra of the intermediate quintet dinitrene and trinitrene **93b** were calculated with the following $\Gamma(E)$ values: 330 MHz (0.011 cm^{-1}) and 180 MHz (0.006 cm^{-1}), respectively.[104] The use of the smaller $\Gamma(E)$ value for calculating the EPR spectrum of trinitrene **93b** was explained by lower rotational mobility of the γ-phenylnitrene moiety due to steric hindrances produces by protons in the β-positions of the pyridine ring. According to quantum chemical calculations, changes in the angles of rotation, ω_1 and ω_3, from 0 to 180° in trinitrene **93b** are accompanied by changes in the D_S and E_S parameters in the ranges of 0.004 and 0.007 cm^{-1}, respectively. A successful analysis of all paramagnetic products of the photolysis of diazide **90** and triazide **92b** laid the basis for the future spectral studies of high-spin oligophenylnitrenes with $S > 3$, *e.g.*, hexanitrene **94** with $S = 6$.

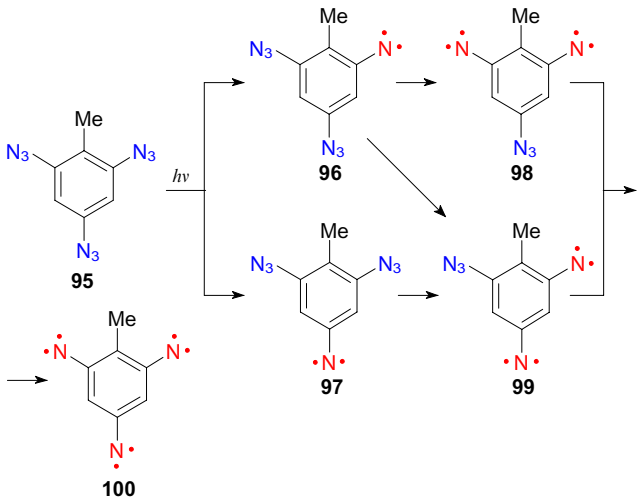
Structure 94



7.3. Septet trinitrenobenzenes

For more than four decades, trinitrene **2** was the sole septet nitrenobenzene reported in the literature. Photolysis of 1,3,5-triazidobenzene-2,4,6-tricarbonitrile in MTHF at 77 K is accompanied by the appearance of numerous signals corresponding to a triplet nitrene with $D_T = 0.9735$ cm^{-1}, $E_T = 0$ and the septet trinitrene **2** with $D_S = -0.0487$ cm^{-1}, $E_S = 0$ in the EPR spectrum.[42] For long, these data were a reference point when evaluating the magnetic parameters of all septet trinitrenes.[1] The second septet nitrenobenzene is trinitrene **100** formed during the photolysis of triazide **95** in different cryogenic matrices (Scheme 14).[105] The EPR spectrum of trinitrene **100** isolated in solid argon at 4 K corresponded to $D_S = -0.0938$ cm^{-1} and $E_S = -0.0040$ cm^{-1} and thus proved that the septet nitrenobenzenes are characterized by much larger (in absolute value) parameters D_S than previously stated. Somewhat different values of the magnetic parameters ($D_S = -0.0934$ cm^{-1}, $E_S = -0.0015$ cm^{-1}) obtained for trinitrene **100** in MTHF solutions at 5 K were due to the formation of molecular complexes between this compound and solvent. An analysis of the parameters D_S and E_S for two matrices showed that complexation of trinitrene **100** with MTHF is accompanied by a decrease in the spin density on the nitrene centres in positions 2 and 6 of the benzene ring by about 4% and by a decrease in the angle Θ between the nitrene C–N bonds of these centres by nearly 2.5°. The energy of long-range spin–spin interactions between the unpaired electrons localized on different nitrene centres was for the first time calculated using the experimentally determined parameter D^{Exp} of trinitrene **100** in argon matrices; this allowed one to assess the efficiency of benzene-1,3,5-triyl core as a linker for spin–spin interactions.

Scheme 14



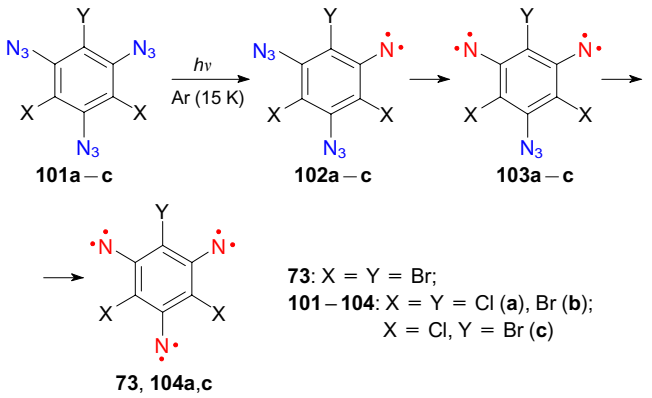
According a theory,[42] the parameter D^{Exp} is the sum of two components, D_{ii} and D_{ij}, where D_{ii} is the total energy of spin–spin interactions between three pairs of unpaired electrons localized on three biradical units and D_{ij} is the total energy of 12 long-range spin–spin interactions between the unpaired electrons separated by the benzene-1,3,5-triyl moiety. The parameter D_{ij} is defined as the difference between the parameters D^{Exp} and D_{ii}, where D_{ii} is calculated using expression (6). According to calculations,[105] for trinitrene **100** one has $D_{ij} = 0.009$ cm^{-1}, which is less than 10% of D^{Exp}. Earlier,[64] it was reported that for trinitrene **44** the parameter D_{ij} is as large as 18% of D^{Exp} owing to more efficient long-range spin–spin interactions between unpaired electrons through the 1,3,5-triazino-2,4,6-triyl moiety.

Using EPR spectroscopy, it was found that the formation of trinitrene **100** during the photolysis of triazide **95** proceeds in nearly quantitative yield assuming that no side diamagnetic products of nitrene insertion into the benzene ring are also formed.[105] As to the intermediates of this reaction, noticeable amounts of only triplet mononitrenes

96 and **97** are formed in the early stages of photolysis. As in the case of production of trinitrene **1**, intermediate quintet dinitrenes **98** and **99** are the most photochemically labile paramagnetic compounds formed during the generation of trinitrene **100**. These two dinitrenes can be detected only at very early stages of photolysis of triazide **95** from the appearance of very weak signals at 301 and 308 mT corresponding to the strongest lines of the X_2-transitions of quintet dinitrenes.

The closest analogue of trinitrene **2** is trinitrene **104a** with D_{3h} symmetry. It can be obtained by photolysis of triazide **101a** in argon at 15 K in almost quantitative yield (Scheme 15).[86, 106] The early stages of photolysis involve the formation of very small amounts of quintet dinitrene **103a**, the only intermediate of this reaction. Weak signals of **103a** in the EPR spectrum appear at 145, 160 and 300 mT.

Scheme 15



Trinitrene **104a** isolated in argon matrices shows $D_S = -0.0957$ cm^{-1} and $E_S = 0$. A salient feature of the X-band EPR spectrum of this trinitrene is the appearance of a strong line of two-photon Z_1-transition at 18 mT (Fig. 5). Its position makes possible highly accurate calculations of the parameter D_S for most trinitrenes with D_{3h} symmetry using Eqn (8):

$$h\nu_0 = |3D_S| + g\beta H_{Z1}\,, \qquad (8)$$

where $h\nu_0$ is the microwave quantum energy of the EPR spectrometer; g is the g-factor ($g \sim 2$); β is the Bohr magneton; and H_{Z1} is the position of the Z_1-transition.[86]

The solution of Eqn (8) for trinitrene **2** using the parameters[42] $h\nu_0 = 9396$ MHz and $H_{Z1} = 42$ mT gave $|D_S| = 0.092$ cm^{-1}. Quantum chemical calculations predicted a similar D_S value for trinitrene **2**.[105] Moreover, computer simulations of the EPR spectrum using the parameters $g = 2.003$, $D_S = -0.092$ cm^{-1} and $E_S = 0$ showed that the simulated spectrum includes all characteristic lines reported for trinitrene **2** and that the pattern of the simulated spectrum closely resembles that of the simulated spectrum of trinitrene **104a** (Fig. 5 *b*).[86]

In addition to EPR spectroscopy, trinitrene **104a** was also studied by UV and IR spectroscopies in different cryogenic matrices including Ar, Ne, Xe, O_2 and H_2 at 3 K and in H_2O at 8–160 K.[107]

The UV spectrum of trinitrene **104a** in an argon matrix exhibits absorption bands with maxima at 204, 221, 237, 283 and 289 nm, and a weak structured band in the region from 310 to 345 nm, composed of five clearly seen components. This pattern is also common to the UV spectra of trinitrene **104a** in O_2, H_2 and H_2O matrices. The theoretical UV spectrum of trinitrene **104a** obtained from (TD)M06-2X/aug-cc-pVTZ calculations includes almost all absorption bands observed in the experimental UV spectrum of this compound. The only exception is the long-wavelength band in the region of 310–345 nm; calculations predict here only one maximum at 337.6 nm. As in the case of triplet and quintet nitrenes, this band corresponds to $\pi \rightarrow$ SOMO transitions. The large hypsochromic shift of this band compared to the corresponding long-wavelength bands in the spectra of triplet (401–434 nm) and quintet (395–422 nm)[94] nitrenes is indicative of an increase in the energies of $\pi \rightarrow$ SOMO transitions from triplet to quintet and then septet nitrenes owing to enhancement of electron-deficient properties of the molecules bearing a large number of unpaired electrons.

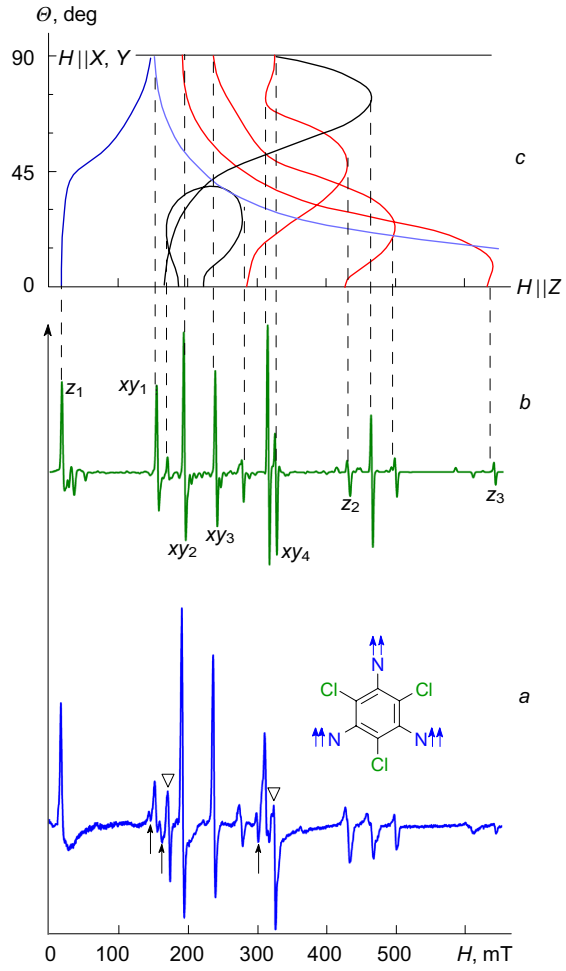
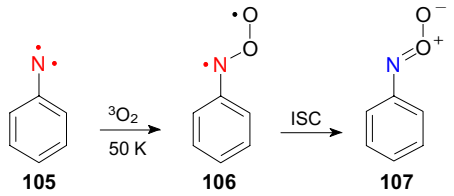


Figure 5. EPR spectrum of trinitrene **104a** in argon matrix. Signals of dinitrene **103a** and signals from impurities in the sapphire rod of the spectrometer are marked by arrows and open triangles, respectively (*a*), simulated EPR spectrum of trinitrene **104a** (*b*) and resonance magnetic fields plotted *vs.* Euler angle Θ (*c*). The plot is based on the data taken from Ref. 86.

According to IR spectroscopy data, photolysis of triazide **101a** in argon matrices produces trinitrene **104a** as the sole product. The formation of **104a** manifests itself in the appearance of five bands at 691, 783, 1131, 1257 and 1330 cm^{-1}.[107] Very weak bands of dinitrene **103a** were observed in neon matrices only, while attempts to detect

the intermediate formation of triplet nitrene **102a** failed for all matrices. The UV spectrum of trinitrene **104a** in water ice matrices remained unchanged up to the onset of matrix sublimation at 160 K, thus demonstrating high thermal stability of this compound. Triplet phenylnitrene **105** isolated in O_2/Xe matrices rapidly reacts with triplet oxygen molecule at 50 K to give a diradical **106**, which is converted to nitroso-*O*-oxide **107** through intersystem crossing (Scheme 16).[108–111] The absence of any changes in the UV spectral pattern of trinitrene **104a** in solid oxygen (20 K) and O_2/Xe (50 K) matrices suggests very high stability of this trinitrene against oxidation by triplet oxygen. Trinitrene **104a** also demonstrated high chemical inertness in solid hydrogen matrices at 3 K, although triplet arylcarbenes almost instantaneously react with hydrogen molecules under identical conditions.[112]

Scheme 16



According to UV and IR spectroscopy data, trinitrene **73** is the sole product of the photolysis of triazide **101b** in argon matrices.[113,114] This trinitrene also does not react with molecular oxygen and molecular hydrogen in O_2, O_2/Xe and H_2 matrices and remains stable up to the onset of water ice matrix sublimation at 160 K.[107] The IR spectrum of trinitrene **73** exhibits a total of five absorption bands at 686, 695, 1113, 1251 and 1316 cm^{-1}.[107] The UV spectrum of this compound demonstrates absorption bands with maxima at 218, 233, and 297 nm, and a weak structured band in the region from 320 to 355 nm. A 10-nm bathochromic shift of the long-wavelength absorption band of trinitrene **73** relative to the corresponding absorption band of trinitrene **104a** suggests a slight decrease in the energies of $\pi \rightarrow$ SOMO transitions in the molecules of high-spin nitrenes owing to the effect of heavy bromine atoms.

According to the X-band EPR spectra shown in Fig. 6 trinitrene **73** has $g = 2.003$, $|D_S| = 0.202$ cm^{-1} and $E_S = 0$. The $|D_S|$ parameter of trinitrene **73** is nearly twice as high as those of all known septet trinitrenes (Fig. 7), being record high for septet organic molecules. Moreover, it is a few

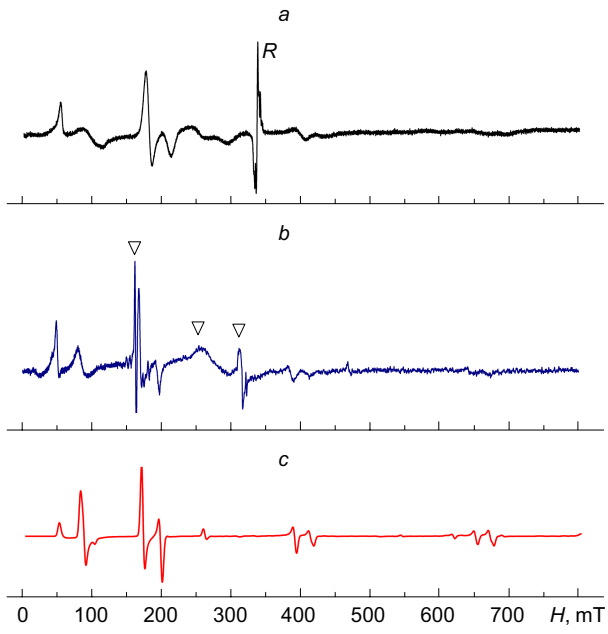


Figure 6. EPR spectrum (9.433 GHz) of trinitrene **73** in methylcyclohexane (MCH) glass (*a*), EPR spectrum (8.889 GHz) of trinitrene **73** in argon matrix (*b*), and simulated EPR spectrum (*c*). Signals from impurities in the sapphire rod of the spectrometer are marked by open triangles. The plot is based on the data taken from Ref. 114.

orders of magnitude higher than those of certain metal-containing septet molecules, *e.g.*, MnH with $D_S = -0.0027$ cm^{-1} and MnF with $D_S = -0.0083$ cm^{-1} (Ref. 1). According to quantum chemical calculations, the D_S parameter of trinitrene **73** should be negative.[86] The results of calculations were in excellent agreement with the W-band EPR spectra (Fig. 8), which allow one to unambiguously determine the signs of the parameters D of high-spin molecules.[114] The spectra demonstrated not only signals of trinitrene **73** with $g = 2.0073$, $D_S = -0.203$ cm^{-1} and $E_S = 0$, but also those of triplet mononitrene **102b** with $g = 2.0033$, $D_T = 1.3692$ cm^{-1} and $E_T = 0.0932$ cm^{-1} and quintet dinitrene **103b** with $g = 2.0070$, $D_Q = -0.3062$ cm^{-1} and $E_Q = 0.0137$ cm^{-1}, which are not observed by the less sensitive X-band EPR spectroscopy.

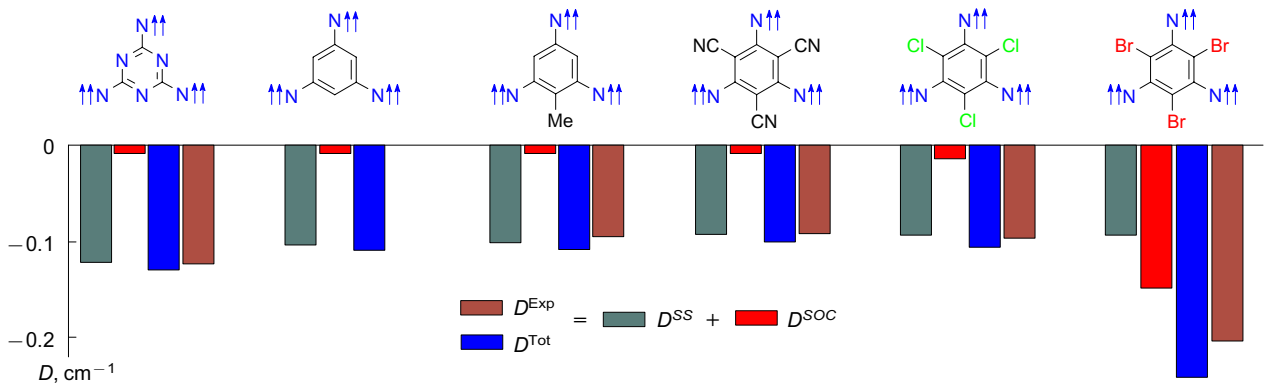


Figure 7. The D^{SS}, D^{SOC}, D^{Tot} and D^{Exp} parameters of different septet trinitrenes. The plot is based on the data taken from Ref. 114.

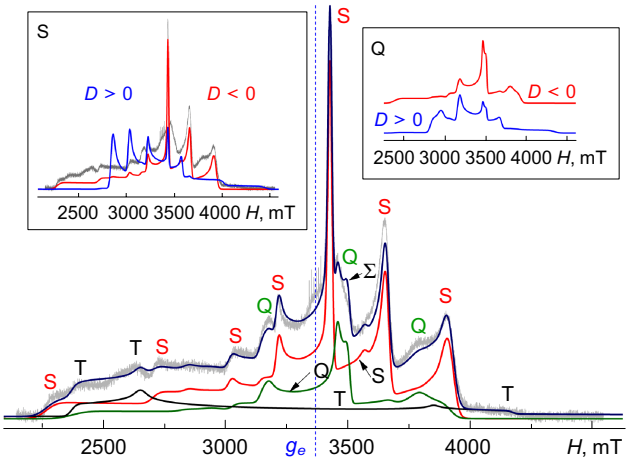


Figure 8. EPR spectrum (93.997 GHz) of products of the photolysis of triazide **101b** in MCH glass. T, Q and S are the simulated spectra of triplet nitrene **102b**, quintet dinitrene **103b** and septet trinitrene **73**, respectively. The plot is based on the data taken from Ref. 114.

The W-band EPR spectra of nitrenes were recorded for the first time. They make it possible to detect the total spectrum of high-spin molecules with large parameters D, which is impossible in the case of low-frequency X-band EPR spectroscopy since many signals of triplet, quintet and septet molecules are beyond the operating magnetic field range from 0 to 1000 mT. Besides, the fact that the W-band EPR spectra of molecules with the parameters D of the same magnitude but opposite signs are fundamentally different allows one to experimentally determine the signs of these parameters (see insets in Fig. 8).

Among all known triplet and septet arylnitrenes, nitrene **102b** and trinitrene **73** have the highest parameters D_T and D_S, respectively; negative sign of the parameter D_Q of quintet dinitrene **103b** was explained by the large contribution of spin–orbit coupling to the $\boldsymbol{D}^{\mathrm{Tot}}$ tensors of these molecules owing to the effect of heavy bromine atoms (Table 7).

Since the molecules of mononitrene **102b** and trinitrene **73** have the same orientation of the principal magnetic axes

Structure 103b

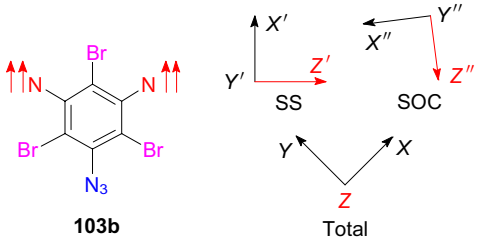


Table 7. Parameters D and E (in cm^{-1}) of nitrenes **102b**, **103b** and **73** obtained from PK-PBE/Ahlrichs-DZ calculations.[114]

Nitrene	S	D^{SS}	D^{SOC}	D^{Tot}	E^{SS}	E^{SOC}	E^{Tot}
102b	1	0.992	0.421	1.413	0.005	0.076	0.081
103b	2	0.196	0.202	−0.331	0.037	0.048	−0.003
73	3	−0.093	−0.147	−0.240	0.000	0.000	0.000

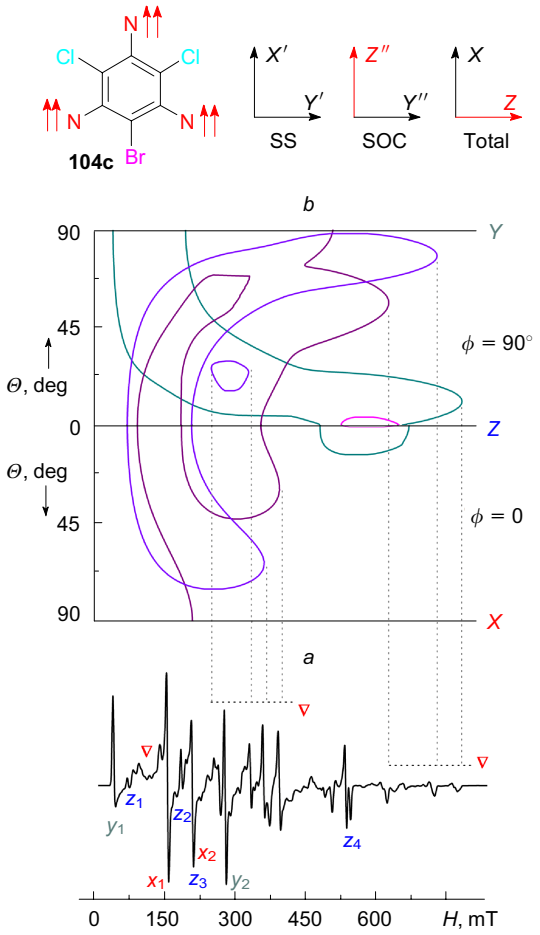


Figure 9. EPR spectrum of trinitrene **104c** (*a*) and resonance magnetic fields plotted *vs.* Euler angles Θ and ϕ (*b*). The plot is based on the data taken from Ref. 115.

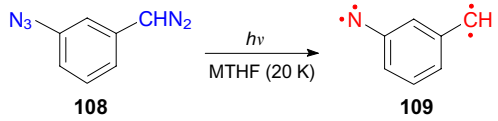
of the tensors $\boldsymbol{D}^{\mathrm{SS}}$ and $\boldsymbol{D}^{\mathrm{SOC}}$, the total tensor $\boldsymbol{D}^{\mathrm{Tot}}$ is the scalar sum of $\boldsymbol{D}^{\mathrm{SS}}$ and $\boldsymbol{D}^{\mathrm{SOC}}$. A dramatically different situation occurs with the molecule of dinitrene **103b** where the principal magnetic axes of the tensors $\boldsymbol{D}^{\mathrm{SS}}$ and $\boldsymbol{D}^{\mathrm{SOC}}$ have different orientations. Diagonalization of these positive tensors gives a negative total tensor $\boldsymbol{D}^{\mathrm{Tot}}$.

According to X-band EPR spectroscopy data, photolysis of triazide **101c** in argon matrix at 15 K yields septet trinitrene **104c** with $D_S = 0.1237$ cm^{-1} and $E_S = 0.0324$ cm^{-1} as the sole product.[115] This compound has an unusual EPR spectrum since the E_S parameter is very high, being close to the maximum value $1/3\,D_S$ (Fig. 9 *a*). A study of trinitrene **104c** showed that septet trinitrenes with one heavy bromine atom in the six-membered aromatic ring are characterized by positive parameter D_S and possess no magnetic bistability. According to *ab initio* CASCI(12,12)/SVP calculations of trinitrene **104c**, the principal magnetic axes of the tensors $\boldsymbol{D}^{\mathrm{SS}}$ (-0.099 cm^{-1}) and $\boldsymbol{D}^{\mathrm{SOC}}$ (-0.164 cm^{-1}) have different orientations and their diagonalization gives a positive total tensor $\boldsymbol{D}^{\mathrm{Tot}}$ ($+0.123$ cm^{-1}).

8. High-spin nitrenocarbenes and nitreno radicals

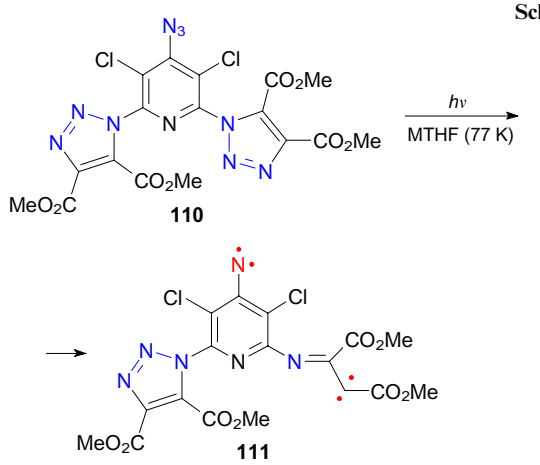
Quintet nitrenocarbene **109** generated during the photolysis of azide **108** in MTHF at 20 K (Scheme 17) is the first high-spin nitrene with $S > 1$ containing radical centres of different nature.[116]

Scheme 17



The EPR spectrum of nitrenocarbene **109** appeared to be much more complicated than that of quintet dinitrene **1**, and it was impossible to exactly determine the parameters D_Q and E_Q without computer simulations. This also holds for the interpretation of the EPR spectrum of quintet nitrenocarbene **111** produced by photolysis of azide **110** in MTHF at 77 K (Scheme 18).[117]

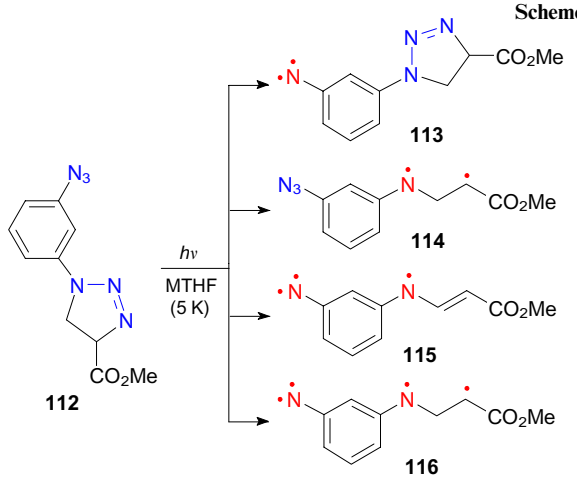
Scheme 18



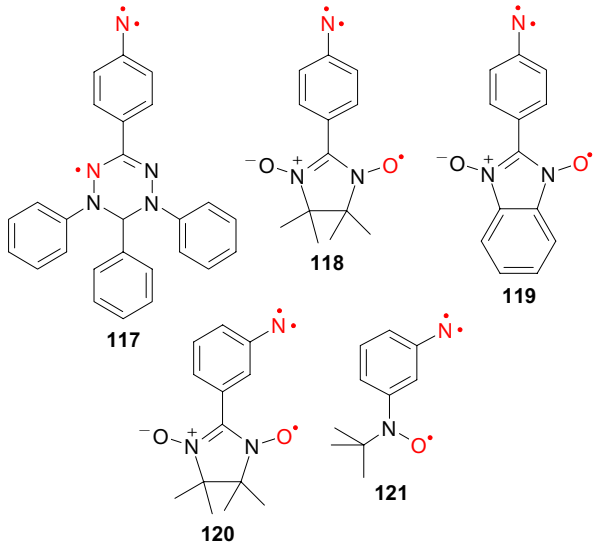
Photolysis of azide **112** in MTHF at 5 K (Scheme 19) produces[118] a mixture of paramagnetic products including two triplet systems, nitrene **113** and diradical **114**, a quartet ($S = 3/2$) nitreno radical **115** and a quintet nitreno diradical **116**. Diradical **116** is the first high-spin nitreno radical system characterized by magnetic parameters. One has $g = 2.003$, $D_Q = 0.170$ cm^{-1} and $E_Q = 0.004$ cm^{-1} for diradical **116** and $g = 2.003$, $D = 0.345$ cm^{-1} and $E = 0.0003$ cm^{-1} for quartet nitreno radical **115**. The EPR signals of both nitreno radicals disappeared at $T > 5$ K.

Quartet nitreno radicals **117**–**121** containing stable free-radical centres were obtained by photolysis of corresponding azides in MTHF at 77 K and characterized by UV and EPR spectroscopies.[119–122] Owing to absorption of verdazyl radical in the regions of 350, 445 and 750 nm[123,124] the

Scheme 19



Structures 117–121



UV spectrum of triradical **117** exhibits a variety of absorption lines with maxima at 360, 450, 545, 590, 680 and 750 nm.[120–122] The long-wavelength absorption bands of triradicals **118**–**121** are observed in the region of 650–680 nm. The magnetic parameters of the triradicals are listed in Table 8.

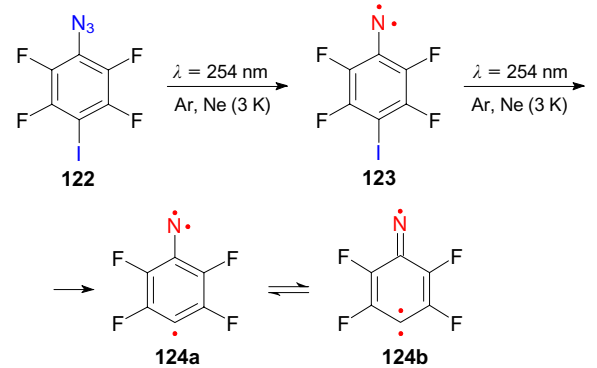
Table 8. Parameters D and E of triradicals **117**–**121**.

Radical	Matrix	$\|D\|$, cm^{-1}	$\|E\|$, cm^{-1}	Ref.
117	MTHF	0.280	0.000	122
118	MTHF	0.263	0.000	122
119	MTHF	0.256	0.000	121
120	MTHF	0.352	0.006	121
121	MTHF	0.336	0.004	121

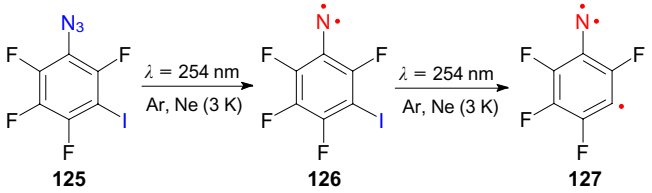
Compounds **124**, **127** and **130** belonging to another class of quartet nitreno radicals were obtained by photolysis of azides **122**, **125** and **128**, respectively, in solid argon and neon matrices at 3 K and characterized by IR and EPR spectroscopies (Schemes 20, 21 and 22).[125–132]

IR spectroscopy studies revealed that triradicals **124**, **127** and **130** have extremely low thermal and photochemical stability and readily undergo rearrangements to various diamagnetic products. The EPR spectra of triradicals **124** and **130** are hardly discernible against the background of the intense spectra of triplet nitrenes **123** and **129**, while the EPR signals from triradical **127** were not observed even in

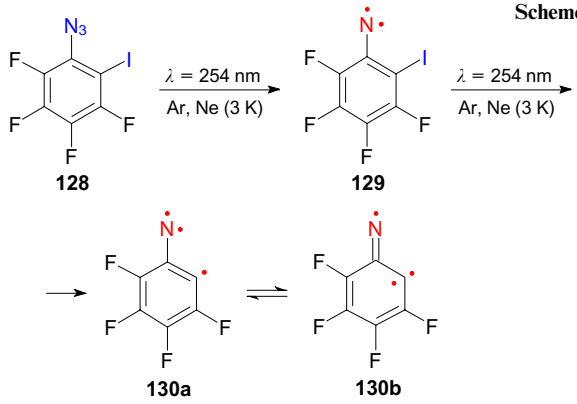
Scheme 20



Scheme 21



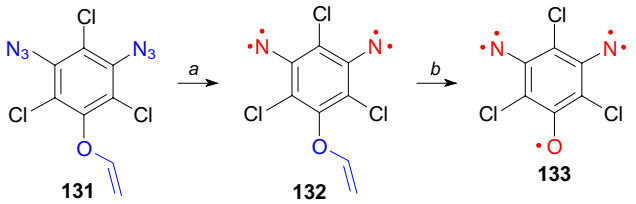
Scheme 22



the neon matrix at 3 K. Higher stability of triradicals **124a** and **130a** was explained by their ability to exist in equilibrium with triradicals **124b** and **130b**. Triradical **124a** is characterized by $g = 2.003$, $D = 0.285$ cm^{-1} and $E = 0.043$ cm^{-1} (*cf.* $g = 2.003$, $D = 0.357$ cm^{-1} and $E = 0.0136$ cm^{-1} for triradical **130a** with a shorter distance between the radical centres).

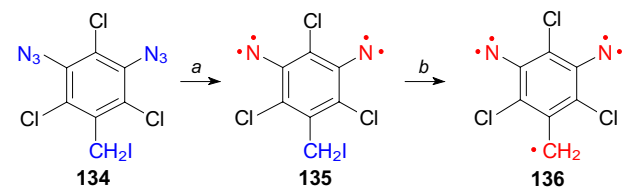
Recently characterized dinitreno radicals **133** (Scheme 23) and **136** (Scheme 24) are the first sextet nitreno radicals ($S = 5/2$).[133] Irradiation of diazides **131** and **134** in MCH glasses at 5 K by long-wavelength light caused generation of quintet dinitrenes **132** ($D_Q = 0.190$ cm^{-1}, $E_Q = 0.043$ cm^{-1}) and **135** ($D_Q = 0.205$ cm^{-1}, $E_Q = 0.041$ cm^{-1}), which were subsequently irradiated by short-wavelength light to produce the sextet nitreno radicals **133** ($D = 0.088$ cm^{-1}, $E = 0.009$ cm^{-1}) and **136** ($D = 0.125$ cm^{-1}, $E = 0.023$ cm^{-1}). These molecules con-

Scheme 23



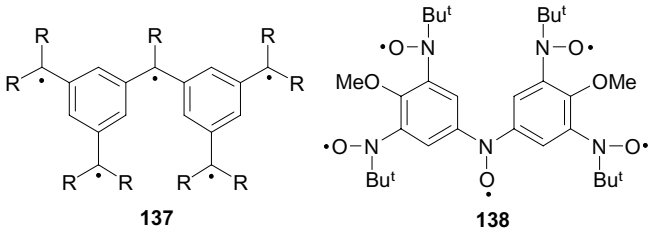
(*a*) $\lambda = 365$ nm, MCH (5 K); (*b*) $\lambda = 254$ nm, MCH (5 K)

Scheme 24



(*a*) $\lambda = 365$ nm, MCH (5 K); (*b*) $\lambda = 254$ nm, MCH (5 K)

Structures 137, 138



R = $C_6H_4Bu^t$-4

tain two biradical nitrene centres each and therefore their parameters D are much higher than those of the sextet pentaradical **137** ($D = 0.027$ cm^{-1}, $E = 0.0009$ cm^{-1})[134] and stable nitroxide pentaradical **138** ($D = 0.0039$ cm^{-1}, $E = 0.0013$ cm^{-1}).[135]

9. Nitrenes and other high-spin organic molecules: a comparison

High-spin polynitrenes considered above belong to a wide class of high-spin organic molecules composed of only light elements (nonmetals), namely, H, C, O, F, N, S, *etc*. Such molecules possess certain common physical properties that are first of all due to the presence of ferromagnetically coupled unpaired electrons. An attractive feature of the molecular structures in question consists in the possibility of being used to design novel metal-free magnetic materials whose physical properties are typical of organic materials, in particular, low density, flexibility and elasticity, a wide transparency window, dielectric properties, *etc*. Traditionally, research into magnetic properties of high-spin organic molecules is based on the idea to design organic ferromagnetic materials representing ensembles of organic molecules or macromolecules with ordered spins (*i.e.*, organic ferro- or ferrimagnetics).[136–138] In the last two decades, new investigation lines of these systems appeared, *e.g.*, research into molecular magnetism[37,53,139] as well as spintronics and quantum informatics.[2–19] In addition to specific physical and chemical problems, a number of common issues concerning magnetic and chemical properties are to be solved. The design of molecular spin ensembles with efficient ferromagnetic interaction between unpaired electrons to stabilize a high-spin state of multispin clusters at room temperature is a challenge. Usually, spin–spin exchange interactions in molecules are described by the Heisenberg–Dirac–van Vleck Hamiltonian (9):

$$H = -\sum\sum J_{ij}S_iS_j \qquad (9)$$

where J_{ij} are the pairwise spin–spin exchange interactions (ferromagnetic at $J > 0$ and antiferromagnetic at $J < 0$).[136,137] A two-spin system with $J > 0$ has a triplet ground electronic state and the energy gap between the triplet ground state ($S = 1$) and excited singlet state ($S = 0$) is $\Delta E_{ST} = 2J$. Assuming an equilibrium Boltzmann population of the two-level system at room temperature ($RT \approx 0.6$ kcal mol^{-1}), the triplet ground state is populated by more than 99% only at $\Delta E_{ST} > 5$ kcal mol^{-1}. Therefore, one should first of all realize ferromagnetic exchange between interacting spins with $J > 2.5$ kcal mol^{-1}.

The design of molecular magnets is based on the synthesis of molecular spin structures with stable high-spin

ground state and slow magnetic relaxation. The energy barrier to magnetic relaxation should be created using anisotropic inter-electron magnetic interactions; traditionally, these are dipole – dipole (spin – spin) interactions and anisotropic spin – orbit coupling, which arises in molecular systems with unquenched orbital angular momentum. Such molecules represent extremely small magnetic domains and can found practical application in various fields including spintronics, quantum informatics, microbiology, *etc*. A key role in solving the problem of molecular magnets is assigned to the parameter D of the ZFS tensor. The barrier to magnetic relaxation (U) appears in systems with negative parameter D and increases with increasing $|D|$ since $U = DS^2$.[53,139] Recent studies showed that the most promising systems for single-molecule magnets (SMM) include mono- and dinuclear organometallic complexes where the barrier to magnetic relaxation is formed involving spin – orbit coupling displayed by the atoms of 3*d*- and 4*f*-metals that have unquenched (or partially quenched) orbital angular momentum in high crystal fields.[140 – 142] Prospects for application of high-spin organic molecules comprising only light elements (nonmetals) cast doubt since the strongest dipole – dipole (spin – spin) interactions provide the $|D|$ values of at most a few reciprocal centimetres. Nevertheless, high-spin organic molecules play an important role in research in this field.[37] They are traditionally used as model systems to gain a better insight into the mechanisms of the onset of anisotropic intramolecular magnetic interactions and to test new methods of quantum chemical computations of both isotropic constants of exchange interactions and anisotropic parameters of the ZFS tensor.[54 – 57]

There are molecular and supramolecular aspects of the design of high-spin organic ensembles. The former deals with elementary building blocks for organic magnets, *viz*., organic molecules bearing unpaired electrons including stable radicals (spin $S = 1/2$) and polyradicals with ferromagnetically interacting unpaired electrons (spin $S \geqslant 1$). At present, a wide variety of suitable radical structures are available. Typical examples of spin molecules with high chemical stability are provided by various nitroxide radicals.[143, 144] In addition, there are quite a few polyradical structures where the energy gap between the high-spin ground state with a total spin of $S \geqslant 1$ and the nearest excited state with the total spin $S-1$ varies over a wide range. They are often used as model systems in studies of the properties of molecular magnets. The supramolecular aspect involves the development of methods for stable ferromagnetic ordering of the spin molecules used as building blocks in crystals or amorphous polymers. Traditionally, the problem is solved using two fundamentally different approaches. One of them is based on McConnell's models, which demonstrate the possibility of ferromagnetic ordering due to intermolecular (through-space) interactions of paramagnetic centres embedded in a crystal. The other approach requires the formation of polyradical structures where ferromagnetic interaction between biradical centres is transferred across the system of π-conjugated bonds (Ovchinnikov's model[145]). In particular, exchange interaction through the benzene ring depends on the mutual arrangement of radical centres. For instance, 1,3-bonding (*meta*-bonding) provides ferromagnetic exchange interactions, whereas 1,4(*para*-) and 1,2(*ortho*)-bonding gives rise to antiferromagnetic interaction and, correspondingly, a singlet ground state.[53] The models are intensively studied both experimentally and theoretically (see reviews[138, 146 – 148]). In this Section we will consider a few typical examples of different molecular structures and compare their characteristics with the magnetic parameters J and $|D|$ of triplet nitrenes and polyradical molecules.

9.1. Main spin units

The most widely used spin units in radical molecules include the triphenylmethyl (**TPM**), nitronyl nitroxide (**NN**), iminoyl nitroxide (**IN**), aminoxyl (**NO**), aminyl (**AM**), thioaminyl (**TAM**), dithiadiazolyl (**DTDA**), phenoxyl (**PhO**), diarylcarbene (**DAC**), verdazyl (**VZ**), oxaverdazyl (**OVZ**), thiaverdazyl (**TVZ**), bisdithiazolyl (**BDTA**), bisdiselenazolyl (**BDSA**) and 1,2,4-benzotriazinyl (**BTA**) fragments.[149 – 153]

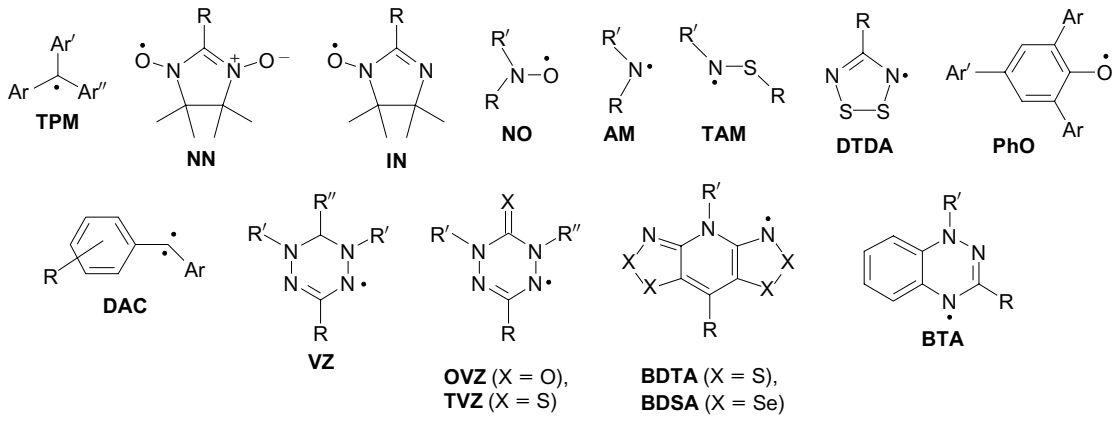
Except **DAC**, all other structural fragments are stable at room temperature and widely used in the design of organic magnetic materials. However, **DAC**-containing polycarbenes are characterized by much higher parameters D and are of considerable interest as convenient models for studying ferromagnetic exchange interactions between biradical centres in structurally complicated multispin macromolecules.[154 – 158]

Aromatic compounds bearing diradical moieties **139 – 142** form a particular class of high-spin organic molecules. Studies on these highly reactive and unstable species also contribute largely to the development of general theory of chemical bonding, structure and reactivity of organic molecules.[159, 160]

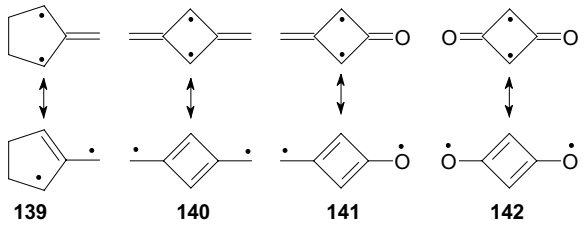
9.2. Spin – spin interactions in triplet diradicals

To date, the ZFS parameters of several hundreds of organic triplet biradicals have been determined. Consideration of such a large data array goes beyond the scope of our review.

Structures of TPM – BTA fragments



Structures 139 – 142



Spin – spin interactions in triplet biradicals have been comprehensively reviewed elsewhere.[149 – 160] The properties of triplet biradicals containing two **TPM**, nitroxide and **VZ** fragments have also been reviewed.[138, 144, 161] In this Section we will restrict ourselves to discussing selected triplet biradicals **143 – 156** chosen to compare the energies of dipole spin – spin interactions between different spin units (Table 9).

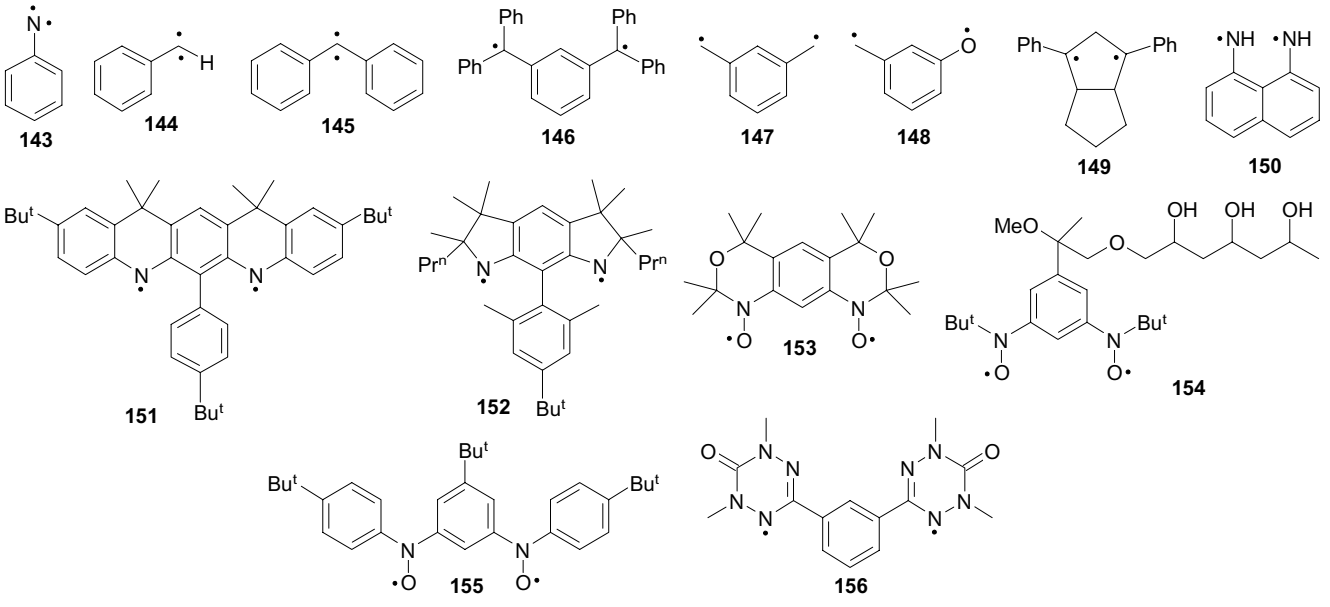
Table 9. Parameters D and E of triplet biradicals **143 – 156**.

Radical	$\|D\|$, cm^{-1}	$\|E\|$, cm^{-1}	Ref.
143	0.9990	0.0000	162
144	0.5150	0.0251	163
145	0.4053	0.0190	164
146	0.0064	0.0006	165
147	0.0110	0.0010	166
148	0.0270	0.0080	167
149	0.0570	0.0005	168
150	0.0270	0.0004	154
151	0.0092	0.0021	169
152	0.0175	0.0036	170
153	0.0130	0.0016	171
154	0.0124	0.0011	172
155	0.0086	0.0013	173
156	0.0063	0.0004	174

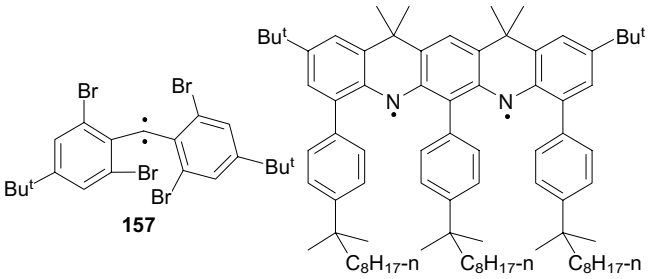
According to theory,[1] the magnitude of the parameter D of triplet biradicals is inversely proportional to the cubed distance between interacting unpaired electrons. Owing to localization of two unpaired electrons on the same atom, nitrene **143** and carbene **144** are characterized by the largest values of the parameters D among the biradicals **143 – 156**. Compared to the carbon atom of carbene **144**, the nitrogen atom of nitrene **143** has a larger positive nuclear charge, a shorter distance between the unpaired electrons and a larger value of the parameter D.[21] Among biradicals **146 – 149**, molecule **149** is characterized by the shortest distance between the unpaired electrons and by the largest parameter D, while the smallest D value was found for biradical **146** where the spin density is delocalized over five aromatic rings. For the same reason the parameter D of carbene **145** is considerably smaller than that of carbene **144**. Much larger values of the parameters D of biradicals **148** and **150** show that the energy of dipole spin – spin interactions in triplet molecules also increases when unpaired electrons are localized on more electronegative atoms. Considering triplet molecules **150 – 156**, the smallest parameter D was found for bis(verdazyl) radical **156**, while the largest one was inherent in the bisaminyl radical **152**. The larger the parameter D the wider the energy gap ΔE_{ST} between the triplet ground and the singlet excited spin states. Triplet arylnitrenes are characterized by $\Delta E_{ST} \gg 30$ kcal mol^{-1}, whereas those of triplet carbenes and bisaminyl, bis(nitroxide), bis(verdazyl) and bis(triarylmethyl) biradicals are respectively $\sim$3, 10, 30 and 40 times smaller.[149 – 154]

Recently, organic triplet biradicals have been used as molecular devices for quantum informatics.[5 – 19] A key step in the device fabrication process involves coating the surface of various substrates (titania, copper, *etc.*) with biradicals; this implies a sufficiently high thermal and chemical stability of the biradicals. Bis(verdazyl) radicals are the least reactive triplet molecules that remain stable on long-term storage in solution and in the solid phase at room temperature.[161] Many triplet bis(nitroxide) radicals containing a bulky substituent or aromatic nucleus at the nitrogen atom in the spin unit N – O have also high kinetic stability.[144] Triplet bis(triarylmethyl) radicals, *e.g.*, diradical **146**, are stabilized through efficient delocalization of the spin density from the radical centre to aromatic moieties.[138] It was Schlenk's discovery of stable diradical **146** in 1915 (see Ref. 175) that gave rise to chemistry of high-spin organic compounds. Considerable advances in stabilizing highly reactive triplet diarylcarbenes made in the last 15 years are based on the use of bulky *tert*-butyl substituents or bromine

Structures 143 – 156



Structures 157, 158



and iodine atoms as protective groups adjacent to the carbene centre.[176] This allowed one to obtain triplet diarylcarbenes **157**, which are stable in solution at room temperature, and to study their molecular structures by single-crystal X-ray diffraction.[177] The synthesis of compound **158** ($D_T = 0.0086$ cm^{-1}, $E_T = 0.00195$ cm^{-1} and $\Delta E_{ST} = 5$ kcal mol^{-1}), the first triplet bisaminyl diradical that is stable in solution at room temperature,[178,179] gave an impetus to studies on the synthesis of stable polyaminyl radicals with $S > 2$. Triplet arylnitrenes bearing the highest spin density on the radical centre and possessing the highest reactivity have lifetimes from 10 ns to 500 ms in solution at room temperature depending on the properties of the aromatic nucleus; amazingly, some of them are highly stable in the solid phase and can even be characterized by X-ray diffraction analysis.[27,180,181] Therefore, it cannot be ruled out that certain triplet arylnitrenes may appear to be promising materials for quantum informatics.

9.3. Spin – spin interactions in quintet tetraradicals

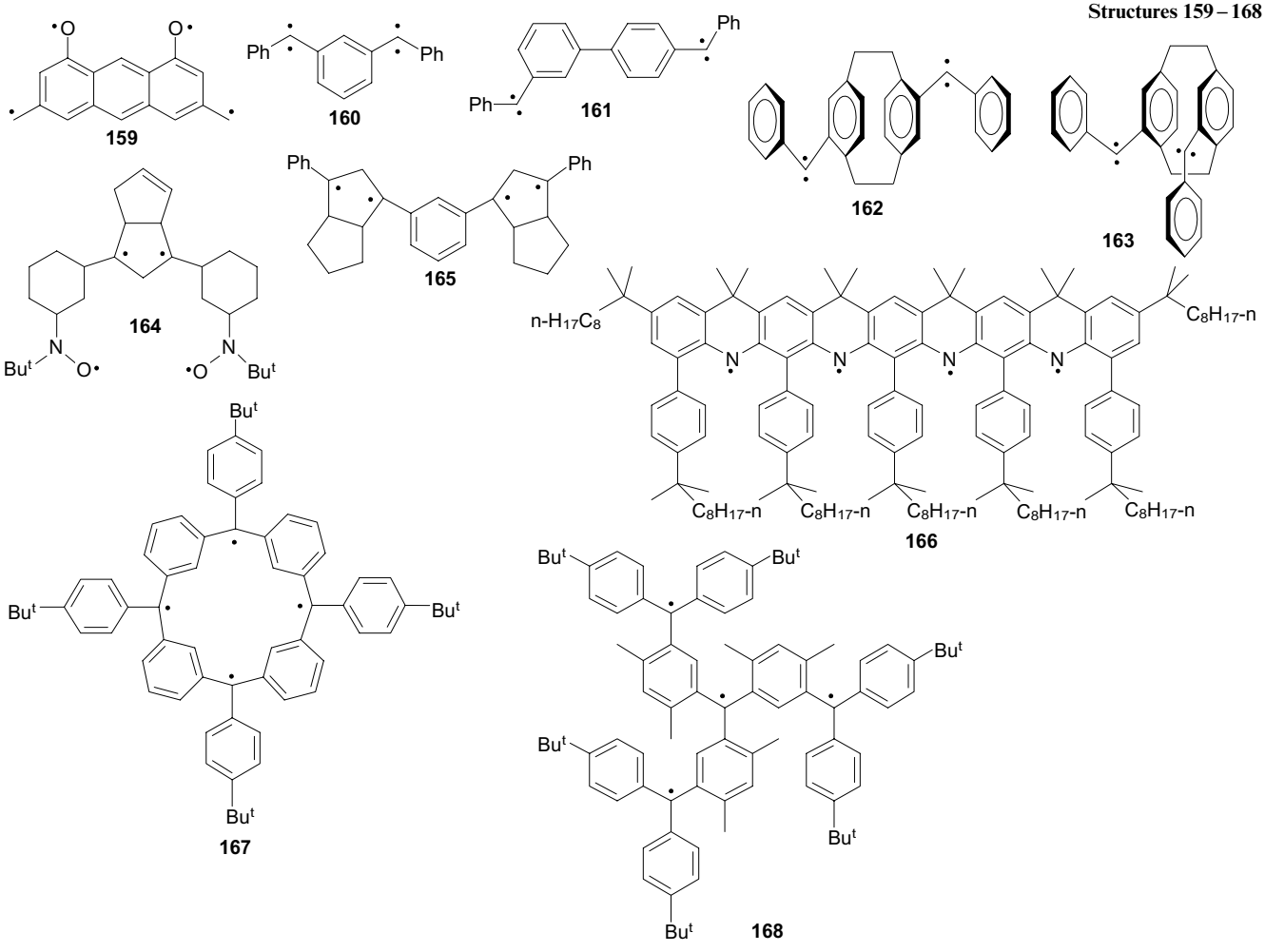
In addition to quintet dinitrenes, several dozens of organic tetraradicals with quintet ground spin state have been reported,[149–154] *e.g.*, tetraradicals **159** – **168** whose magnetic parameters D and E are listed in Table 10.

Among the systems **159** – **168**, quintet dicarbenes **161** and **162** with *E*-arranged PhC moieties have the largest parameters D. Isomeric conditionally *Z*-dicarbenes **160** and **163** with lower symmetry have almost halved parameters D and much larger parameters E. As to tetraradicals **159**, **164**

Table 10. Parameters D and E of quintet tetraradicals **150** – **168**.

Radical	$\lvert D\rvert$, cm^{-1}	$\lvert E\rvert$, cm^{-1}	Ref.
159	0.0117	0.0032	154
160	0.0713	0.0190	182
161	0.1256	0.0058	183
162	0.1215	0.0085	184
163	0.0624	0.019	184
164	0.0127	0.0014	185
165	0.0096	0.0029	168
166	0.0052	0.0016	178
167	0.0033	0.0000	134
168	0.0069	0.0000	186

Structures 159 – 168



and **165**, the last-mentioned system has the smallest parameter D since all the four unpaired electrons are localized on the least electronegative carbon atoms. Tetraaminyl radical **166** and tetra(triarylmethyl) radicals **167** and **168** have the smallest parameters D, especially, tetraradical **167** with a calix[4]arene structure. A SQUID magnetometry study showed that the energy gap ΔE_{QT} between the quintet ground and triplet excited spin states of quintet tetraradical **166** exceeds 150 K ($\sim$0.3 kcal mol^{-1}).[178]

Similarly to triplet diradicals, most quintet tetraradicals are characterized by positive parameters D and do not exhibit the fundamental properties of molecular magnets. The only exception is recently reported quintet dinitrene **103b** with $D_Q = -0.3062$ cm^{-1} and a spin-inversion barrier of 1.225 cm^{-1} ($\sim$1.5 K) between the W_{-2} and W_{+2} states.[114]

9.4. Spin – spin interactions in septet hexaradicals

The magnetic parameters D and E of only five non-nitrene organic septet molecules **169** – **173** are available in the literature. The ZFS parameters of these molecules are listed in Table 11.

Table 11. Parameters D and E of septet hexaradicals **169** – **173**.

Radical	$\|D\|$, cm^{-1}	$\|E\|$, cm^{-1}	Ref.
169	0.04158	0.01026	187
170	0.06670	0.00045	188
171	0.00907	0.00019	189
172	0.01500	0.00100	190
173	0.04000	0.00500	191

The D and E parameters of septet tricarbenes **169** and **170** were determined from the EPR spectra of UV-irradiated single crystals grown by co-crysallization of corresponding diazo precursors with benzophenone.[187, 188] The ZFS parameters of septet hexaradicals **171** – **173** were determined form the EPR spectra of products of the photolysis of diazo precursors in MTHF glasses at 4 – 77 K.[189 – 191] The septet molecules **169** – **173** are characterised by negative parameters D and exhibit the properties of molecular magnets. The spin-inversion barriers separating the W_{-3} and W_{+3} states of these systems are very low and vary from 0.10 to 0.45 K [*cf.* 1.33 K and 2.19 K for the septet trinitrenes **44** ($D = -0.123$ cm^{-1})[64] and **101b** ($D = -0.2032$ cm^{-1})[114] respectively].

9.5. Organic polyradicals with $S > 3$

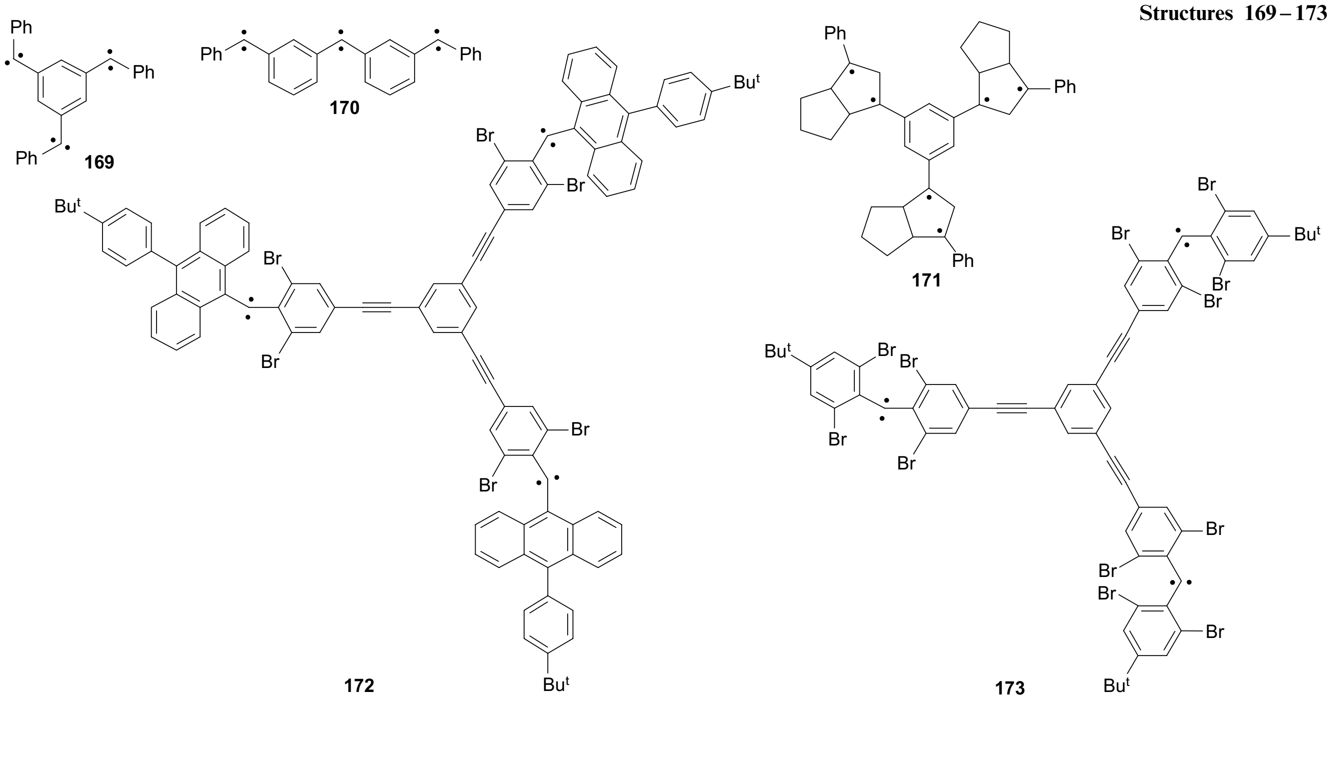
Among all classes of organic polyradicals with $S > 3$, the D and E parameters are known for two nonet organic octaradicals (**174**, **175**), one octet heptaradical (**176**) and two undecet decaradicals (**177** and **178**) (Table 12). The D parameter of nonet tetracarbene **174** containing four biradical centres is twice as high as that of the nonet octaradical **175**. However, an increase in the spin state to $S = 5$ causes the differences in D to decrease, as follows from the data for oligoradicals **177** and **178**.

Table 12. Parameters D and E of polyradicals **174** – **178** c $S > 3$.

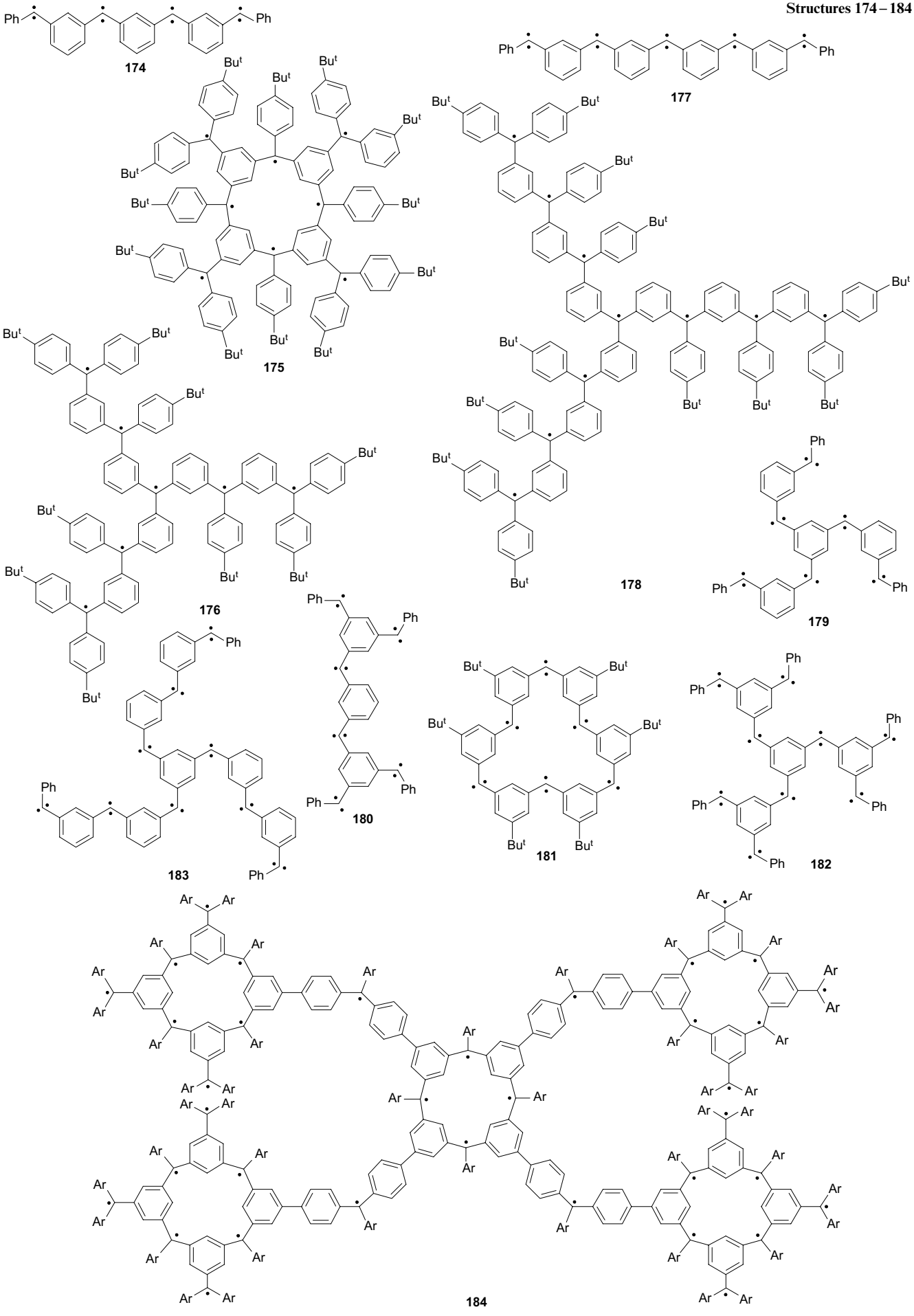
Radical	S	$\|D\|$, cm^{-1}	$\|E\|$, cm^{-1}	Ref.
174	4	0.0332	0.0031	192
175	4	0.0127	0.0000	134
176	7/2	0.0027	0.0001	193
177	5	0.0168	0.0036	194
178	5	0.0120	0.0000	193

According to EPR spectroscopy and magnetometry studies, the nonet tetracarbene **174** and undecet pentacarbene **177** are formed in quantitative yield during the photolysis of the parent oligodiazo compounds and have the spin states $S = 4$ and $S = 5$, respectively.[192, 194] However, attempts to generate linear oligocarbenes with six ($S = 6$) and seven ($S = 7$) carbene centres failed due to inefficient photolysis of six and seven diazomethane units in the precursor molecules.[194] Tridecet hexacarbenes were

Structures 169 – 173



Structures 174 – 184

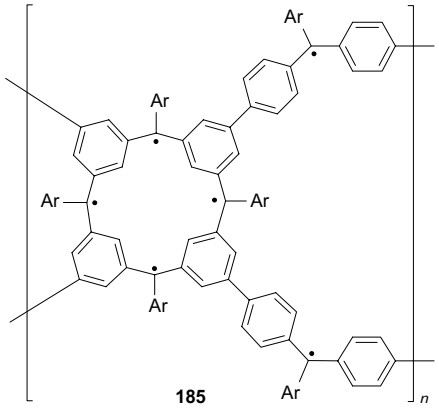


synthesized only for structurally more rigid compounds **179**–**181** with $S = 6$, as followed from magnetometry data.[195,196] An attempt to generate nonacarbene **182** by photolysis of corresponding diazo precursor led only to oligocarbene with seven carbene centres and $S = 7$.[197] At the same time, magnetic measurements confirmed that structurally different nonacarbene **183** has $S = 9$.[198] This is the highest experimentally detected spin state of oligocarbenes.

Organic polyradicals with the highest spin state are based on macrocyclic triarylmethyl radicals. Synthetic routes to such systems and methods of investigation of their magnetic properties have been thoroughly analyzed in a review.[138] A record high spin state ($S = 13$) of the polyradical **184** containing 36 radical centres was detected experimentally.[199] This polyradical possessed interesting magnetic properties, *viz*., high saturation magnetization ($M_{sat} = 0.6\ \mu_B$) and magnetic susceptibility ($\chi T_{max} = 86\ cm^3\ K\ mol^{-1}$).

Calixarene-based spin units were used to prepare a cross-linked polymer **185** with a molecular mass in the range of 300 000–500 000 and $S = 3000$–7000.[200] The polymer exhibited the properties of a supermagnet, namely, the spin-inversion barrier was ~15 K at $T < 10$ K, while the total spin S was as high as nearly 5000, thus being indicative of rather high degree of magnetic ordering of radical centres in the polymer molecule. Polymer **185** still remains a top notch in the design of organic magnetic materials.

Structure 185



185

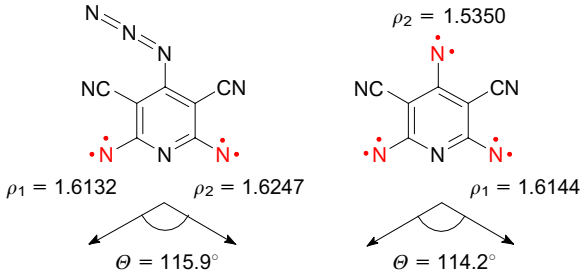
10. Quantum chemical calculations of high-spin nitrenes

Quantum chemical calculations play a key role in studies of high-spin nitrenes since none of them can be isolated in pure form and characterized by conventional analytical methods. Therefore, identification of high-spin nitrenes is solely based on comparison of experimental and simulated UV, IR and EPR spectra while a proper choice of computational method plays a decisive role. Quantum chemical calculations are also carried out to determine the energy gaps between the spin states of multispin molecules, their geometric parameters and spin densities on biradical centres, which are then used to evaluate the energies of spin–spin interactions from Eqns (3)–(7). Different tasks are solved using different theoretical approaches.

10.1. Calculations of IR spectra, geometric parameters and spin density

As long as two decades ago a comparison of the experimental IR spectra of quintet dinitrenes **61a** and **69b**,**c** and septet trinitrenes **72b**,**c** in argon matrices at 7 K with the results of conventional quantum chemical calculations at a UB3LYP/6-31G* level of the density functional theory (DFT) with a scale factor of 0.961 revealed a reasonable agreement between the experiment and theory.[76] Density functional calculations were also successfully used in studies of IR spectra of dinitrenes **1**, **43**, **69a**, **76b**,**c** and septet trinitrenes **44** and **72a**.[64,84,94] At present, the IR spectra of high-spin nitrenes are calculated using an improved computational method M06-2X/aug-cc-pVTZ.[107]

Structures 69c, 72c



69c **72c**

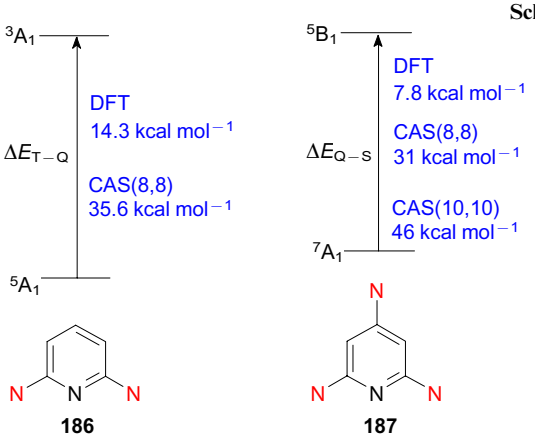
Note that the UB3LYP/6-31G* and UB3LYP/6-311+G** methods employed to predict the IR spectra of quintet and septet nitrenes are at least equally suitable for the determination of their structural parameters and spin densities, ρ_N, on the nitrene centres.[51,52,79,80] For instance, the D parameters of molecules **69c** and **72c** determined using Eqns (4)–(7) with the Θ and ρ_N values obtained from UB3LYP/6-311+G** calculations agreed with the D values found from the corresponding EPR spectra to an accuracy of 99% and 95%, respectively.[80]

Only one study on the energy gaps between the high-spin ground and low-spin excited states of quintet and septet nitrenes has been reported to date.[46] Based on the results of UB3LYP/6-31G* calculations, it was shown that the quintet ground spin state $^5A_2$ of dinitrene **186** lies 14.3 kcal mol^{-1} lower than its excited state $^3A_1$ on the energy scale (Scheme 25). *Ab initio* CASSCF-(8,8)/6-31G*//CASSCF(8,8)/6-31G* calculations increased the energy gap between the $^5A_2$ and $^3A_1$ states of dinitrene **186** to 35.6 kcal mol^{-1}. The septet ground spin state $^7A_2$ and the quintet excited state $^5B_2$ of trinitrene **187** are separated by slightly narrower energy gaps (see Scheme 25). However, calculations at a CASSCF(10,10)/6-31G*//CASSCF(8,8)/6-31G level of theory [in abbreviated form CAS(10,10) and CAS(8,8), respectively] predict a larger value of 46 kcal mol^{-1} for the energy gap between the $^7A_2$ and $^5B_2$ states of trinitrene **187**. So wide energy gaps between the high-spin ground and low-spin excited states were reported for no other organic radicals with quintet or septet ground spin states.

10.2. Calculations of UV spectra

The UV spectrum of quintet dinitrene **76b** isolated in solid argon, which was recorded in 2003,[94] still remains the only known electronic absorption spectrum of individual organic

Scheme 25



quintet tetraradical. A theoretical analysis of this spectrum by *ab initio* multiconfigurational quasi-degenerate second-order perturbation theory calculations MCQDPT2//CASSCF(16,12)//UB3LYP/6-311G** using the active space with 16 electrons and 12 orbitals was reported in 2006.[74] The key findings of this study are summarized in Table 13 and in Scheme 26. It was found that MCQDPT2//CASSCF(16,12)//UB3LYP/6-311G** calculations can describe the electronic absorption spectra of quintet molecules with reasonable accuracy.

The electronic absorption spectra of septet organic hexaradicals **73** and **104a** isolated in solid argon at 3 K were for the first time reported in 2019.[107] The UV spectra of septet trinitrenes **73** and **104a** were theoretically analyzed using the time-dependent density functional (TD)M06-2X and the aug-cc-pVTZ basis set. In most cases, the results of (TD)M06-2X/aug-cc-pVTZ calculations of nitrenes and other high-spin molecular systems are well comparable with the experiment.[107, 201, 202] The results of studies on the UV spectra of septet trinitrenes **73** and **104a** are summarized in Table 14 and in Fig. 8.

The UV spectra of trinitrenes **73** and **104a** demonstrate an interesting feature, *viz.*, a vibrational fine structure of the long-wavelength absorption band in the region of 310–355 nm (Fig. 10).[107] This absorption band corresponds to the $n_s \rightarrow p_y$ transition of electrons on the nitrene centres, while the vibrational fine structure of these transitions is indicative of the formation of several vibrational states among the excited electronic states of trinitrenes **73** and **104a**.

Table 13. Electronic transitions of quintet dinitrene **76b** (argon matrix).[74]

Transition	Experiment		Calculations	
	λ, nm	A [a]	λ, nm	f [b]
$0.69(4a'' \rightarrow 6a'') - 0.51(6a'' \rightarrow 7a'')$	422	0.006	409	0.009
$0.65(4a'' \rightarrow 5a'') - 0.50(5a'' \rightarrow 7a'')$	418	0.006	393	0.005
$0.90(22a' \rightarrow 26a')$	337	0.022	333	0.018
$0.43(3a'' \rightarrow 6a'') - 0.34(6a'' \rightarrow 8a'')$	320	0.066	321	0.002
$0.25(4a'' \rightarrow 6a'') - 0.47(6a'' \rightarrow 7a'')$	288	0.065	269	0.093
$0.42(5a'' \rightarrow 8a'')$	268	0.051	268	0.066
$0.47(3a'' \rightarrow 6a'') - 0.57(6a'' \rightarrow 8a'')$	239	0.072	233	0.089

[a] Absorption intensity. [b] Oscillator strength.

Scheme 26

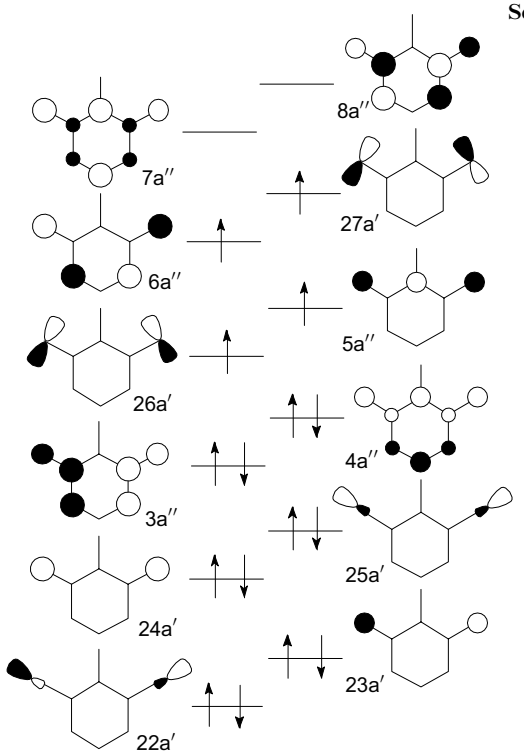
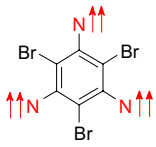
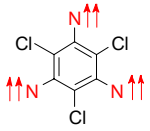


Table 14. UV spectroscopic data for septet trinitrenes **73** and **104a** (argon matrix).[107]

Nitrene	Experiment		Calculations	
	λ, nm	A [a]	λ, nm	f [b]
 **73**	320–355	w	338.9	0.005
	315	w	301.2	0.006
	297	m	277.2	0.117
	233	s	220.8	0.267
	218	vs	203.6	0.023
			201.1	0.109
 **104a**	310–345	w	337.6	0.005
	289	w	293.9	0.009
	283	w	286.7	0.024
	237	w	252.9	0.045
	221	vs	214.6	0.387
	204	m	208.6	0.066

[a] Absorption intensity: w stands for weak, m stands for medium, s stands for strong and vs stands for very strong. [b] Oscillator strength.

Good agreement between the experimental and theoretically calculated UV spectra of trinitrenes **73** and **104a** shows that DFT calculations using the properly chosen hybrid functionals and basis sets provide a reasonably accurate description of excited electronic states of high-spin organic molecules. This conclusion is substantiated by the analysis of modern theoretical methods for calculations of UV spectra of different compounds.[203]

10.3. Calculations of zero-field splitting parameters

Quantum chemical calculations of the ZFS parameters of arylnitrenes were for the first time reported in 2008 taking

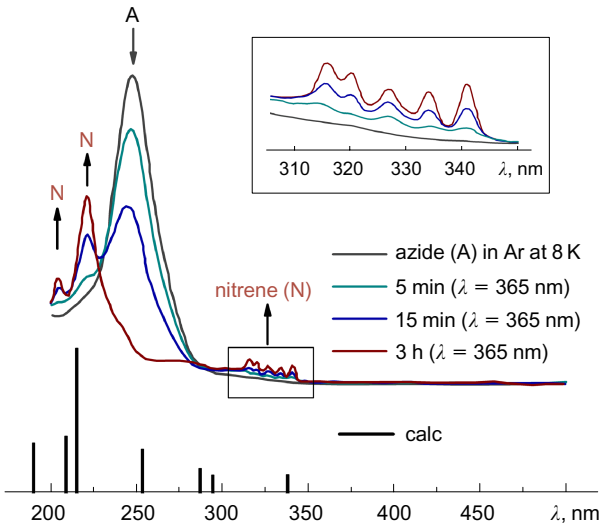


Figure 10. Experimental and simulated UV spectra of septet trinitrene **104a**.[107] This Figure is courtesy of John Wiley and Sons.

the quartet nitreno radical **124** as an example.[128] These were DFT calculations using the B3LYP hybrid functional and the TZVPP basis set incorporated into the ORCA software package. This method quite correctly reproduced the parameter D (0.261 cm^{-1}) of nitreno radical **124** in argon matrices; however, the E parameter (0.017 cm^{-1}) was strongly underestimated (*cf.* experimentally measured values $D = 0.285\ cm^{-1}$ and $E = 0.043\ cm^{-1}$). To find more efficient methods for accurate calculations of the ZFS parameters of high-spin nitrenes, both pure density functionals (BP, BLYP, PBE) and the hybrid density functional B3LYP and different basis sets (DZ, TZV, SVP, EPR-II, EPR-III and 6-311 + G**) were tested in 2010 in relation to triplet nitrenes **60b**, **66b**, **68b**, quartet nitreno radical **124**, quintet dinitrenes **61b**, **69b**, **70b** and septet trinitrenes **44**, **72a**,**b** and **100** with known experimental ZFS parameters in argon matrices.[58] The best results for nitrenes with $S = 1$, 3/2, 2 and 3 were obtained only using the pure functionals BP, BLYP and PBE, which include the spin polarization effects in the nitrene molecules characterized by strong delocalization of the spin density from the nitrene centres to aromatic moieties. For instance, BLYP/EPR-II calculations of the ZFS parameters of quartet nitreno radical **124** predicted $D = 0.310\ cm^{-1}$ and $E = 0.044\ cm^{-1}$. Modern *ab initio* calculations[204] of this system gave similar results. Test DFT calculations of the ZFS parameters of nitrenes also showed that the size of the basis sets has almost no effect on the accuracy of calculations. The maximum deviations of the calculated D and E parameters of nitrenes obtained using different pure functionals are at most 9% and 2%, respectively.[58] The most accurate values of the ZFS parameters were obtained from PK-PBE/Ahlrichs-DZ (or PBE/DZ) calculations, which are now used in all studies of high-spin nitrenes.[66, 81 – 83, 86, 113 – 115] High accuracy of this method is illustrated in Table 1 in relation to the theoretically calculated parameters D and E of quintet dinitrene **47a** (difference between theory and experiment is only 3%).[66] When PK-PBE/Ahlrichs-DZ calculations are used to predict the ZFS parameters of high-spin nitrenes in frozen organic solutions, the solvent effects are included within the framework of the conductor-like screening model (COSMO).[103, 104]

Table 15. ZFS parameters (in cm^{-1}) of trinitrene **104c**.[115]

Parameter	Calculations		Experiment
	PK-PBE/ Ahlrichs-DZ	CASCI(12,12)/ SVP	
D^{SS}	−0.094	−0.094	–
D^{SOC}	0.131	−0.164	–
D^{Total}	0.177	0.123	|0.124|
$(E/D)^{Total}$	0.180	0.260	|0.262|

For most high-spin nitrenes containing heavy atoms the accuracy of PK-PBE/Ahlrichs-DZ calculations of the ZFS parameters somewhat decreases.[57, 115, 205] The possibility of reliable theoretical analysis of the ZFS parameters of high-spin molecules containing heavy atoms using *ab initio* calculations was demonstrated taking bromine-substituted trinitrene **104c** as an example (Table 15).[115]

11. Possible application fields of high-spin molecules

For long, high-spin nitrenes remained the least studied class of high-spin organic polyradicals due to high values of the parameters D and strong delocalization of the spin density in the molecules. Researchers turned their attention to these compounds only after the development of modern software for studying organic molecular magnetism. In particular, before 1996 all experimental methods for the determination of the ZFS parameters of high-spin polyradicals were based on simulations of the EPR spectra using the semiempirical SimFonia-Bruker program that proved itself for high-spin molecular systems with $D_Q < 0.01\ cm^{-1}$.[168] The need for accurate determination of the ZFS parameters of molecules with $S > 2$ and high parameters D gave an impetus to the development of new-generation software EigenfieldMethod (1994),[206] X-Sophe (1999),[207] SIM-ESR (2002),[208] and EasySpin (2006)[48] based on exact numerical solution to the spin Hamiltonian (1). The first tests of all these programs involved an analysis of the EPR spectra of high-spin organic molecules taking quintet dinitrene **35**,[43] septet trinitrene **44** (Ref. 64) and quintet dinitrenes **61a**,**b** (Ref. 50) and **1** as respective examples.[97]

High-spin nitrenes also played a prominent role in developing quantum chemical methods for calculating the ZFS parameters and electronic absorption spectra of high-spin molecules. Taking high-spin nitrenes as examples, it was established that DFT calculations of the ZFS parameters of strongly polarized high-spin organic molecules should be carried out using pure density functionals and small basis sets, *e.g.*, the PK-PBE/Ahlrichs-DZ combination.[58] The results of quantum chemical calculations of the electronic absorption spectra of quintet dinitrene **76b**[74] and septet trinitrenes **73** and **104a**[107] demonstrated that modern computational methods can rather accurately evaluate parameters of excited states of high-spin organic molecules with $S = 2$ and 3.

To date, none of the known organic radicals with $S > 2$ has found practical application. The same also holds for all known organometallic SMM and single-ion magnets (SIM) despite the fact that they have high spin-inversion barriers

and high blocking temperature (> 80 K) and are chemically stable.[4] For instance, the first SMM (complex $[Mn_{12}O_{12}(CH_3COO)_{16}(H_2O)_4]$, or simply Mn_{12} in abbreviated form; prepared in 1993) is characterized by $S = 10$, $D = -0.46$ cm^{-1} and a barrier of U of 46 cm^{-1} (50 K) separating the W_{-10} and W_{+10} states.[209] Nevertheless, for certain reasons neither Mn_{12} nor other SMM and SIM materials have found practical application.[4,53] The most interesting feature of molecular multispin systems is their potential of being materials for quantum computers.[2–20] In external magnetic field, a molecule bearing an unpaired electron ($S = 1/2$) becomes a two-level spin system (Zeeman splitting) where transitions between the energy levels can be triggered by electromagnetic pulses.[2] Such a two-level spin system is the smallest building block for data processing and storage in quantum computer (so-called qubit).[2–5] Unlike the classical computer where a bit can access two discrete states $|0\rangle$ and $|1\rangle$, a qubit is a superposition of the states $|0\rangle$ and $|1\rangle$, which is described as

$$|\psi\rangle = A|0\rangle + B|1\rangle \qquad (10)$$

where A and B are the complex amplitudes of the states, which obey the condition $|A|^2 + |B|^2 = 1$.[5] The main challenge in quantum computing is to design qudits representing a wealth of qubits.[4] For instance, a three-qubit qudit can simultaneously handle 2^3 states. It was reported that a quantum computer with a qudit handling a total of 50 qubits should outperform all classical supercomputers available at the moment.[2,4] Numerous attempts to design quantum computers based on organometallic SMM and SIM faced severe difficulties associated with the onset of strong noise from various effects, such as superfine and quadrupole interactions between electron spins and atomic nuclei of metals and ligand atoms, lattice thermal vibrations, appearance of photons, isotopic effects, *etc*.[4] To eliminate the undesirable effects, molecules of organometallic SMM and SIM are placed in highly dilute media (one SMM or SIM molecule per 10000 magnetically inactive molecules). However, this approach by default excluded the possibility of integrating individual qubits and thus prepare multuqubit qudits. Starting with 2016, multispin molecules and complexes representing multiqubit quantum registers have attracted considerable attention of researchers in the field of design of quantum computers based on spin systems.[4] An essential requirement for the multispin systems is that they should be characterized by relatively small ZFS values (usually, less than 0.4 cm^{-1}) for convenient manipulation of spin transitions. Recently, a SIM of the composition $[GdP_5W_{30}O_{110}]^{12-}$ with $S = 7/2$ and $D = -0.124$ cm^{-1}, representing an eight-level quantum qudit composed of three qubits, has been studied.[210] This three-qubit qudit remains the largest among all SMM and SIM tested to date. It can handle eight states $|000\rangle$, $|001\rangle$, $|011\rangle$, $|010\rangle$, $|110\rangle$, $|100\rangle$, $|101\rangle$ and $|111\rangle$ and a large number of different-type quantum gates. In principle, it cannot be ruled out that certain high-spin organic molecules can also act as quantum qudits. Unfortunately, the vast majority of high-spin organic polyradicals are lack structural rigidity, which is required for generating noise-free signals. The most rigid molecular structure is inherent only in mononuclear high-spin nitrenes characterized by appropriate values of the parameter D and strong polarization necessary to integrate individual molecules into a large quantum register.[20] An example of a seven-level quantum qudit based on trinitrene **72b** ($S = 3$, $D = -0.102$ cm^{-1}) isolated in solid argon is shown in Fig. 11.

The experimental 9.107-GHz EPR spectrum of trinitrene **72b** randomly oriented in solid argon exhibits fifteen lines corresponding to the allowed single-photon canonical Z-, X- and Y-transitions (five lines for each principal axis) and two strongest lines of two-photon Z-transitions, which eventually corresponds to a 17-qubit system. The number and intensities of resonance transitions can be varied using pulsed EPR spectroscopy and different frequencies, phases and polarization of microwave radiation. A key parameter of a qubit is the lifetime of the state $|1\rangle$ being generated, or the coherence time (T_2). The longest coherence time $T_2 = 700$ ms (at 4 K) was reported for the $[V^{IV}(C_8S_8)_3]^{2-}$ SIM.[4] Meanwhile, studies on the dependence of the EPR signal intensity on the microwave power showed that the coherence time T_2 of high-spin nitrenes isolated in crystals of the parent azides can be as long as tens of seconds at

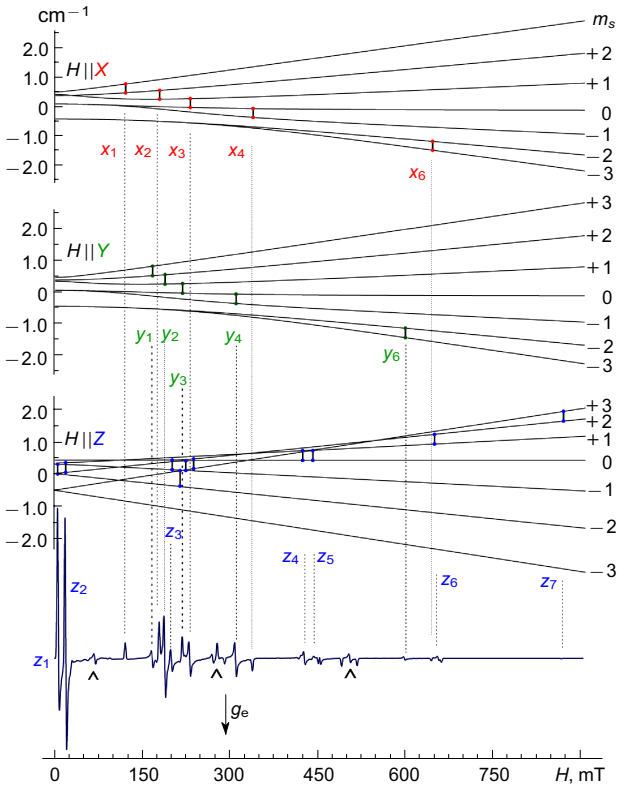
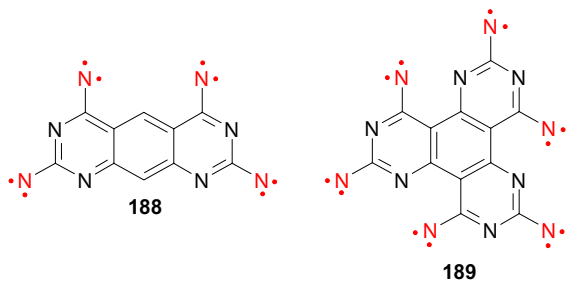


Figure 11. Simulated EPR spectrum of septet trinitrene **72b** and calculated Zeeman energy levels. The plot is based on the data taken from Ref. 52.

Structures 188, 189



77 K.[89,93] Therefore, recently generated, thermally and chemically stable septet trinitrenes **73** and **104a** may appear to be rather promising for the development of at least prototypes of quantum computers. It should also be noted that new high-spin nitrenes are much cheaper and simpler to synthesize than new SMM and SIM based on lanthanides, whose magnetic properties are often difficult to predict *a priori*. For instance, tetranitrene **188** with $S = 4$ and hexanitrene **189** with $S = 6$ (see Ref. 20) are technologically relatively accessible, whereas the design of a SMM- (or SIM)-based high-spin system with identical spin topology and properties seems to be hardly possible.

12. Conclusion

Although the first EPR spectra of quintet dinitrene **1** and septet trinitrene **2** were detected more than five decades ago, experimental and theoretical studies of high-spin nitrenes began only recently after the development of public-domain software for computer simulation of EPR spectra and angular dependences of resonance magnetic fields for any high-spin molecules in 2006,[48] and after the development of software for quantum chemical calculations of spin – spin interactions and spin – orbit coupling in polyradicals in 2008.[49] Within a short period of time, dozens of different quintet and septet nitrenes were synthesized (generated) and a rigorous mathematical description of the interplay between the molecular structures and magnetic properties of this class of high-spin molecules was developed. Studies on aryldi- and trinitrenes were accompanied by the detection, for the first time, of the UV and IR spectra of organic molecules with quintet and septet ground spin states. It was found that septet trinitrenes with *sym*-triazine skeleton and pyrimidinylnitrenes are characterized by the strongest spin – spin interactions among organic hexaradicals, also being photochemically unstable, and photochemical generation of these molecules is accompanied by their decomposition to low-molecular-mass fragments. The major drawback of most septet pyridinyltrinitrenes consists in low yield ($< 10\%$) during the photolysis of the parent triazides. The only exception is septet difluoro-substituted trinitrene **72a**, which is formed nearly quantitatively. The D_S parameter of compound **72a** is -0.1018 cm^{-1}, being about 50-fold higher than those of septet organic hexaradicals and certain metal-containing molecules, *e.g.*, MnH and MnF. Among all septet trinitrenes, the most practically interesting properties are possessed by perhalo-substituted trinitrenobenzenes. They are formed quantitatively during the photolysis of triazides, are the most photochemically and thermally stable, inert towards molecular oxygen and hydrogen and have high negative parameters D_S. For instance, septet trinitrene **73** is characterized by the highest negative parameter $D_S = -0.203$ cm^{-1} among all known septet organic molecules.

Research into high-spin nitrenes allowed one not only to obtain new organic magnetic compounds, but also to discover and study a number of important physical regularities that are of considerable independent interest. These are (i) the effect of heavy atoms on the magnitude and sign of the magnetic anisotropy of organic magnetic molecules, (ii) dependence of the electronic absorption spectra on the ground spin state of polyradicals and (iii) selectivity of photolysis of nonequivalent $N-N_2$ bonds in aromatic polyazides.

Compared to metal-containing SMM, organic SMM are less chemically stable and characterized by much lower blocking temperatures and spin-inversion barriers separating the W_{-S} and W_{+S} spin states.[149–152] A great advantage of organic SMM is their relative simplicity, which excludes a complicated analysis of Coulomb and exchange interactions between *d*- and *f*-electrons and makes it possible to develop simpler algorithms for quantum switches of spin states for quantum informatics.[211–214] In addition, the current rapid progress in new technologies does not exclude that it is SMM with relatively low spin-inversion barriers that may appear to be in high demand for quantum informatics and the problem of stabilizing solid organic SMM at room temperature will be solved successfully.

The review has been written with the financial support from the Russian Foundation for Basic Research within the framework of the Expansion Programme (Project No. 19-13-50194). The authors express their gratitude to the Institute of Problems of Chemical Physics, Russian Academy of Sciences, for providing access to bibliographic and abstract databases and to full-text access to domestic and international scientific journals (within the framework of the State Assignment AAAA-A19-119070790003-7 and AAAA-A19-119092390079-8).

The list of notations used in the review is as follows:

β — Bohr magneton;

$\Gamma(E)$ — line broadening parameter of the spin Hamiltonian for E parameters;

$\Gamma(D)$ — line broadening parameter of the spin Hamiltonian for D parameters;

Θ — angle between the nitrene C – N bonds in di- and trinitrene molecules;

ρ — spin density;

ρ_{NQ} — spin density on the nitrene centre of quintet dinitrene;

ρ_{NT} — spin density on the nitrene centre of triplet mononitrene;

D — zero-field splitting parameter of fine-structure levels for molecules with $S > 1/2$;

D_S, D_Q, D_T — zero-field splitting parameters D of fine-structure levels for septet, quintet and triplet molecules, respectively;

D_t — zero-field splitting parameter D of fine-structure levels for triplet biradical centres in molecules of quintet and septet nitrenes;

D^{SS} — calculated contribution of spin – spin interactions to the parameter D;

D^{SOC} — calculated contribution of spin – orbit coupling to the parameter D;

D^{Tot} — calculated total contribution of spin – spin interactions and spin – orbit coupling to the parameter D;

D^{Exp} — experimentally measured parameter D;

DFT — density functional theory;

E — zero-field splitting parameter of fine-structure levels for molecules with $S > 1/2$;

E_S, E_Q, E_T — zero-field splitting parameters E of fine-structure levels for septet, quintet and triplet molecules, respectively;

EPR — electron paramagnetic resonance;

g — g-factor of radical;

g_e — g-factor of an electron;

Gy — Gray;

$H_{s=n}$ — Hamiltonian of a spin system in the spin state $S = n$, where $n > 1/2$;

H — external magnetic field strength,
J — exchange parameter;
J_{ij} — exchange parameter for exchange between electrons i and j;
K — Kelvin;
m_S — spin quantum number,
MCH — methylcyclohexane,
MTHF — 2-methyltetrahydrofuran,
n^* — number of atoms in the molecule with α-spin density (↑),
n^0 — number of atoms in the molecule with β-spin density (↓);
S — spin angular momentum (vector);
S_x, S_y, S_z — components of the spin angular momentum of the system along the Z, X and Y axes, respectively;
SIM — single-ion magnet;
SMM — single-molecule magnet;
T — Tesla;
W_0, $W_{\pm1}$, $W_{\pm2}$, $W_{\pm3}$ — fine-structure energy sublevels;
X, Y, Z — principal magnetic axes of spin system;
x, y, z — eigenvalues of zero-field splitting tensor;
ZFS — zero-field splitting (ZFS).

References

1. W.Weltner Jr. *Magnetic Atoms and Molecules*. (New York: Dover Publications, 1989)
2. R.Sessoli. *ACS Cent. Sci.*, **1**, 473 (2015)
3. J.M.Zadrozny, J.Niklas, O.G.Poluektov, D.E.Freedman. *ACS Cent. Sci.*, **1**, 488 (2015)
4. A.Gaita-Arino, F.Luis, S.Hill, E.Coronado. *Nat. Chem.*, **11**, 301 (2019)
5. X.Zhang, H.O.Li, G.Cao, M.Xiao, G.C.Guo, G.P.Guo. *Natl. Sci. Rev.*, **6**, 944 (2019)
6. R.Kakavandi, A.Calzolari, Y.B.Borozdina, P.Ravat, T.Chassé, M.Baumgarten, M.B.Casu. *Nano Res.*, **9**, 3515 (2016)
7. F.Ciccullo, A.Calzolari, K.Baser, P.Neugebauer, N.M.Gallagher, A.Rajca, J.vanSlageren, M.B.Casu. *ACS Appl. Mater. Interfaces*, **11**, 1571 (2019)
8. F.Troiani, M.Affronte. *Chem. Soc. Rev.*, **40**, 3119 (2011)
9. J.S.Miller. *Chem. Soc. Rev.*, **40**, 3266 (2011)
10. K.Bader, D.Dengler, S.Lenz, B.Endeward, S.-D.Jiang, P.Neugebauer, J.vanSlageren. *Nat. Commun.*, **5**, 5304 (2014)
11. A.Fernandez, E.Moreno Pineda, C.A.Muryn, S.Sproules, F.Moro, G.A.Timco, E.J.L.Meinnes, R.E.P.Winpwenny. *Angew. Chem., Int. Ed.*, **54**, 10858 (2015)
12. A.Fernandez, J.Ferrando-Soria, E.Moreno Pineda, F.Tuna, I.J.Victorica-Yrezabal, C.Knappke, J.Ujima, C.A.Muryn, G.A.Timco, P.E.Barran, A.Ardavan, R.E.P.Winpwenny. *Nat. Commun.*, **7**, 10240 (2016)
13. M.Shiddiq, D.Komijani, Y.Duan, A.Gaita-Arinõ, E.Coronado, S.Hill. *Nature (London)*, **531**, 348 (2016)
14. F.Ciccullo, N.M.Gallagher, O.Geladari, T.Chassé, A.Rajca, N.B.Casu. *ACS Appl. Mater. Interfaces*, **8**, 1805 (2016)
15. M.Mas-Torrent, M.Crivillers, V.Mugnaini, I.Ratera, C.Rivira, J.Veciana. *J. Mater. Chem.*, **19**, 1691 (2009)
16. K.Sato, S.Nakazawa, R.Rahimi, T.Ise, S.Nishida, T.Yoshino, N.Mori, K.Toyota, D.Shiomi, Y.Yakiyama, Y.Morita, N.Kitagawa. *J. Mater. Chem.*, **19**, 3739 (2009)
17. M.Rohling, G.Burkard. *New J. Phys.*, **14**, 083008 (2012)
18. D.M.Zajac, A.J.Sigillito, M.Russ, F.Brjans, J.M.Taylor, G.Burkard, J.R.Petta. *Science*, **359**, 439 (2018)
19. Y.Xu, D.Awschalom, J.Nitta. *Handbook of Spintronics*. (Dordrecht: Springer, 2016)
20. S.V.Chapyshev. In *Targets in Heterocyclic Systems: Chemistry and Properties*. (Società Chimica Italiana, 2019). Vol. 23, p. 53
21. E.Wasserman. *Prog. Phys. Org. Chem.*, **8**, 319 (1971)
22. B.Iddon, O.Meth-Cohn, E.F.V.Scriven, H.Suschitzky, P.T.Gallager. *Angew. Chem., Int. Ed.*, **18**, 900 (1979)
23. E.F.V.Scriven, K.Turnbull. *Chem. Rev.*, **88**, 297 (1988)
24. M.F.Budyka, M.M.Kantor, M.V.Alfimov. *Russ. Chem. Rev.*, **61**, 25 (1992)
25. N.P.Gritsan, E.A.Pritchina. *Russ. Chem. Rev.*, **61**, 500 (1992)
26. S.Bräse, C.Gil, K.Knepper, V.Zimmermann. *Angew. Chem., Int. Ed.*, **44**, 5188 (2005)
27. N.P.Gritsan, M.S.Platz. *Chem. Rev.*, **106**, 3844 (2006)
28. N.P.Gritsan. *Russ. Chem. Rev.*, **76**, 1136 (2007)
29. M.F.Budyka. *Russ. Chem. Rev.*, **77**, 709 (2008)
30. C.Wentrup. *Angew. Chem., Int. Ed.*, **57**, 11508 (2018)
31. W.Lwowski. *Nitrenes*. (New York: Wiley, 1970)
32. C.Wentrup. *Reactive Molecules*. Wiley, New York, 1984
33. E.F.V.Scriven. *Azides and Nitrenes, Reactivity and Utility*. (New York: Academic Press, 1984)
34. S.Brase, K.Banert. *Organic Azides: Synthesis and Applications*. (Chichester: Wiley, 2010)
35. D.E.Falvey, A.D.Gudmundsdottir. In *Wiley Series of Reactive Intermediates in Chemistry and Biology. Nitrenes and Nitrenium Ions*. Vol. 6. (Hoboken: Wiley, 2013). P. 593
36. P.M.Lahti, M.Minato, C.Ling. *Mol. Cryst. Liq. Cryst.*, **271**, 147 (1995)
37. P.M.Lahti. *Magnetic Properties of Organic Materials*. (New York: Marcel Dekker, 1999)
38. S.V.Chapyshev. *Russ. Chem. Bull.*, **60**, 1274 (2011)
39. S.V.Chapyshev. *Molecules*, **20**, 19142 (2015)
40. G.Smolinsky, E.Wasserman, W.A.Yager. *J. Am. Chem. Soc.*, **84**, 3220 (1962)
41. E.Wasserman, R.W.Murray, W.A.Yager, A.M.Trozzolo, G.Smolinsky. *J. Am. Chem. Soc.*, **89**, 5076 (1967)
42. E.Wasserman, K.Schueller, W.A.Yager. *Chem. Phys. Lett.*, **2**, 259 (1968)
43. T.A.Fukuzawa, K.Sato, A.S.Ichimura, T.Kinoshita, T.Takui, K.Itoh, P.M.Lahti. *Mol. Cryst. Liq. Cryst.*, **272**, 253 (1996)
44. R.D.Kalgutkar, P.M.Lahti. *J. Am. Chem. Soc.*, **119**, 4771 (1997)
45. R.D.Kalgutkar, P.M.Lahti. *Tetrahedron Lett.*, **44**, 2625 (2003)
46. S.V.Chapyshev, R.Walton, J.A.Sanborn, P.M.Lahti. *J. Am. Chem. Soc.*, **122**, 1580 (2000)
47. N.Oda, T.Nakai, K.Sato, D.Shiomi, M.Kozaki, K.Okada, T.Takui. *Synth. Met.*, **121**, 1840 (2001)
48. S.Stoll, A.J.Schweiger. *J. Magn. Reson.*, **178**, 42 (2006)
49. F.Neese. *Comput. Mol. Sci.*, **2**, 73 (2012)
50. S.V.Chapyshev, P.M.Lahti. *J. Phys. Org. Chem.*, **19**, 637 (2006)
51. E.Ya.Misochko, A.V.Akimov, S.V.Chapyshev. *J. Chem. Phys.*, **128**, 124504 (2008)
52. E.Ya.Misochko, A.V.Akimov, S.V.Chapyshev. *J. Chem. Phys.*, **129**, 174510 (2008)
53. J.Cirera, E.Ruiz, S.Alvarez, F.Neese, J.Kortus. *Chem. – Eur. J.*, **15**, 4078 (2009)
54. S.Sinnecker, F.Neese. *J. Phys. Chem. A*, **110**, 12267 (2006)
55. C.Riplinger, J.P.Y.Kao, G.M.Rosen, V.Kathirvelu, G.R.Eaton, S.S.Eaton, A.Kutaladze, F.Neese. *J. Am. Chem. Soc.*, **131**, 10092 (2009)
56. D.V.Korchagin, A.V.Akimov, A.Savitsky, S.V.Chapyshev, S.M.Aldoshin, E.Y.Misochko. *J. Phys. Chem. A*, **122**, 8931 (2018)
57. K.Sugisaki, K.Toyota, D.Shiomi, M.Kitagawa, T.Takui. *Phys. Chem. Chem. Phys.*, **16**, 9171 (2014)
58. E.Ya.Misochko, D.V.Korchagin, K.V.Bozhenko, S.V.Chapyshev, S.M.Aldoshin. *J. Chem. Phys.*, **133**, 064101 (2010)
59. K.Sugisaki, K.Toyota, K.Sato, D.Shiomi, M.Kitagawa, T.Takui. *ChemPhysChem.*, **11**, 3146 (2010)
60. K.Sugisaki, K.Toyota, K.Sato, D.Shiomi, M.Kitagawa, T.Takui. *Phys. Chem. Chem. Phys.*, **13**, 6970 (2011)
61. R.M.Moriarty, M.Rahman. *J. Am. Chem. Soc.*, **88**, 842 (1966)

62. T.Nakai, K.Sato, D.Shiomi, T.Takui, K.Itoh, M.Kozaki, K.Okada. *Mol. Cryst. Liq. Cryst.*, **334**, 157 (1999)
63. T.Sato, A.Narazaki, Y.Kawaguchi, H.Niino, G.Bucher. *Angew. Chem., Int. Ed.*, **42**, 5206 (2003)
64. T.Sato, A.Narazaki, Y.Kawaguchi, H.Niino, G.Bucher, D.Grote, J.J.Wolff, H.H.Wenk, W.Sander. *J. Am. Chem. Soc.*, **126**, 7846 (2004)
65. S.V.Chapyshev, E.N.Ushakov, P.Neuhaus, W.Sander. *J. Org. Chem.*, **79**, 6047 (2014)
66. S.V.Chapyshev, D.V.Korchagin, P.Costa, W.Sander. *J. Photochem. Photobiol., A*, **377**, 207 (2019)
67. J.Cernicharo, M.Guelin, J.R.Pardo. *Astrophys. J. Lett.*, **615**, L145 (2004)
68. S.V.Chapyshev, R.Walton, P.M.Lahti. *Mendeleev Commun.*, **10**, 7 (2000)
69. S.V.Chapyshev, R.Walton, P.R.Serwinski, P.M.Lahti. *J. Phys. Chem. A.*, **108**, 6643 (2004)
70. S.V.Chapyshev, R.Walton, P.M.Lahti. *Mendeleev Commun.*, **10**, 114 (2000)
71. S.V.Chapyshev. *Russ. Chem. Bull.*, **55**, 1593 (2006)
72. E.Ya.Misochko, A.V.Akimov, V.F.Lavitskii, S.V.Chapyshev. *Russ. Chem. Bull.*, **56**, 2364 (2007)
73. S.V.Chapyshev. *Mendeleev Commun.*, **12**, 168 (2002)
74. K.Sugisaki, K.Toyota, K.Sato, D.Shiomi, T.Takui. *Angew. Chem., Int. Ed.*, **45**, 2257 (2006)
75. C.Wentrup. *Acc. Chem. Res.*, **44**, 393 (2011)
76. S.V.Chapyshev, A.Kuhn A., M.W.Wong, C.Wentrup. *J. Am. Chem. Soc.*, **122**, 1572 (2000)
77. S.V.Chapyshev, V.F.Lavitskii, A.V.Akimov, E.Ya.Misochko, A.V.Shastin, D.V.Korchagin, G.V.Shilov, S.M.Aldoshin. *Russ. Chem. Bull.*, **57**, 524 (2008)
78. A.Sasaki, L.Mahé, A.Izouka, T.Sugawara. *Bull. Chem. Soc. Jpn.*, **71**, 1259 (1998)
79. S.V.Chapyshev, D.Grote, C.Finke, W.Sander. *J. Org. Chem.*, **73**, 7045 (2008)
80. S.V.Chapyshev, P.Neuhaus, D.Grote, W.Sander. *J. Phys. Org. Chem.*, **23**, 340 (2010)
81. E.Ya.Misochko, A.V.Akimov, A.A.Masitov, D.V.Korchagin, S.V.Chapyshev. *J. Chem. Phys.*, **137**, 064308 (2012)
82. S.V.Chapyshev, D.V.Korchagin, P.Neuhaus, W.Sander. *Beilstein J. Org. Chem.*, **9**, 733 (2013)
83. S.V.Chapyshev, D.V.Korchagin, D.Grote, W.Sander. *Magn. Reson. Chem.*, **57**, 472 (2019)
84. C.Finke, D.Grote, R.W.Seidel, S.V.Chapyshev, W.Sander. *J. Phys. Org. Chem.*, **25**, 486 (2012)
85. S.V.Chapyshev, R.Walton, P.M.Lahti. *Mendeleev Commun.*, **10**, 187 (2000)
86. E.Ya.Misochko, A.V.Akimov, A.A.Masitov, D.V.Korchagin, S.M.Aldoshin, S.V.Chapyshev. *J. Chem. Phys.*, **138**, 204317 (2013)
87. R.B.Morgunov, V.L.Berdinskii, M.V.Kirman, Y.Tanimoto, S.V.Chapyshev. *High Energy Chem.*, **41**, 33 (2007)
88. S.I.Kuzina, A.I.Mikhailov, S.V.Chapyshev. *High Energy Chem.*, **41**, 245 (2007)
89. S.I.Kuzina, A.I.Mikhailov, S.V.Chapyshev. *Dokl. Phys. Chem.*, **412**, 34 (2007)
90. S.V.Chapyshev, S.I.Kuzina, A.I.Mikhailov. *Mendeleev Commun.*, **17**, 207 (2007)
91. S.I.Kuzina, A.I.Mikhailov, S.V.Chapyshev, D.V.Korchagin, G.V.Shilov, S.M.Aldoshin. *Russ. J. Phys. Chem. A*, **82**, 1870 (2008)
92. S.I.Kuzina, D.V.Korchagin, G.V.Shilov, S.V.Chapyshev, A.I.Mikhailov, S.M.Aldoshin. *Dokl. Phys. Chem.*, **418**, 7 (2008)
93. S.I.Kuzina, S.V.Tokarev, D.V.Korchagin, G.A.Kolpakov, D.V.Khudyakov, S.V.Chapyshev, A.I.Mikhailov, V.A.Nadtochenko, S.M.Aldoshin. *Russ. Chem. Bull.*, **62**, 255 (2013)
94. S.V.Chapyshev, H.Tomioka. *Bull. Chem. Soc. Jpn.*, **76**, 2075 (2003)
95. N.P.Gritsan, Z.Zhu, C.M.Hadad, M.S.Platz. *J. Am. Chem. Soc.*, **121**, 1202 (1999)
96. A.Maltsev, T.Bally, M.L.Tsao, M.S.Platz, A.Kuhn, M.Vosswinkel, C.Wentrup. *J. Am. Chem. Soc.*, **126**, 237 (2004)
97. S.V.Chapyshev. *Russ. Chem. Bull.*, **55**, 1126 (2006)
98. T.Koto, K.Sugisaki, K.Sato, D.Shiomi, K.Toyota, K.Itoh, E.Wasserman, P.M.Lahti, T.Takui. *Appl. Magn. Reson.*, **37**, 703 (2010)
99. S.Sasaki, H.Iwamura. *Chem. Lett.*, 1759 (1992)
100. H.Oka, Y.Miura, Y.Teki. *Mol. Cryst. Liq. Cryst.*, **334**, 41 (1999)
101. Y.Miura, H.Oka, Y.Teki. *Bull. Chem. Soc. Jpn.*, **74**, 385 (2001)
102. N.Oda, T.Nakai, K.Sato, D.Shiomi, M.Kozaki, K.Okada, T.Takui. *Mol. Cryst. Liq. Cryst.*, **376**, 501 (2002)
103. S.V.Chapyshev, D.V.Korchagin, M.F.Budyka, T.N.Gavrishova, P.Neuhaus, W.Sander. *J. Phys. Chem. A*, **115**, 8419 (2011)
104. S.V.Chapyshev, D.V.Korchagin, M.F.Budyka, T.N.Gavrishova, P.Neuhaus, W.Sander. *ChemPhysChem.*, **13**, 2721 (2012)
105. S.V.Chapyshev, E.Ya.Misochko, A.V.Akimov, V.G.Dorokhov, P.Neuhaus, D.Grote, W.Sander. *J. Org. Chem.*, **74**, 7238 (2009)
106. E.Ya.Misochko, A.V.Akimov, A.A.Masitov, D.V.Korchagin, S.V.Chapyshev. *Russ. Chem. Bull.*, **61**, 2218 (2012)
107. E.Mendez-Vega, J.Mieres-Perez, S.V.Chapyshev, W.Sander. *Angew. Chem., Int. Ed.*, **58**, 12994 (2019)
108. J.Mieres-Perez, E.Mendez-Vega, K.Velappan, W.Sander. *J. Org. Chem.*, **80**, 11926 (2015)
109. J.Liu, C.M.Hadad, M.S.Platz. *Org. Lett.*, **7**, 549 (2005)
110. E.A.Pritchina, N.P.Gritsan, T.Bally. *Phys. Chem. Chem. Phys.*, **8**, 6970 (2006)
111. R.L.Safiullin, S.L.Khursan, E.M.Chainikova, V.T.Danilov. *Kinet. Catal.*, **45**, 640 (2004)
112. E.Mendez-Vega, M.Maehara, A.H.Raut, J.Mieres-Perez, M.Tsuge, Y.-P.Lee, W.Sander. *Chem. – Eur. J.*, **24**, 18801 (2018)
113. E.Ya.Misochko, A.V.Akimov, A.A.Mazitov, D.V.Korchagin, I.K.Yakushchenko, S.V.Chapyshev. *Russ. Chem. Bull.*, **64**, 87 (2015)
114. A.Akimov, A.Masitov, D.Korchagin, S.Chapyshev, E.Misochko, A.Savitsky. *J. Chem. Phys.*, **143**, 084313 (2015)
115. E.Ya.Misochko, A.A.Masitov, A.V.Akimov, D.V.Korchagin, S.V.Chapyshev. *J. Phys. Chem. A*, **119**, 2413 (2015)
116. H.Tukada, K.Mutai, H.Iwamura. *Chem. Commun.*, 1159 (1987)
117. S.V.Chapyshev, R.Walton, P.M.Lahti. *Mendeleev Commun.*, **10**, 138 (2000)
118. H.Tukada. *Org. Lett.*, **3**, 3261 (2001)
119. P.M.Lahti, B.Esat, R.Walton. *J. Am. Chem. Soc.*, **120**, 5122 (1998)
120. P.M.Lahti, B.Esat, Y.Liao, P.Serwinski, J. Lan, R.Walton. *Polyhedron*, **20**, 1647 (2001)
121. P.Serwinski, B.Esat, P.M.Lahti, Y.Liao, R.Walton, J. Lan. *J. Org. Chem.*, **69**, 5247 (2004)
122. T.L.Allen, P.M.Lahti. *J. Phys. Chem. A*, **115**, 4922, (2011)
123. P.V.Petunin, E.A.Martynenko, M.E.Trusova, M.S.Kazantsev, T.V.Rybalova, R.R.Valiev, M.N.Uvarov, E.A.Mostovich, P.S.Postnikov. *Eur. J. Org. Chem.*, 4802 (2018)
124. P.V.Petunin, T.V.Rybalova, M.E.Trusova, M.N.Uvarov, M.S.Kazantsev, E.A.Mostovich, L.Postulka, P.Eibisch, B.Wolf, M.Lang, P.S.Postnikov, M.Baumgarten. *ChemPlusChem*, **85**, 159 (2020)

125. H.H.Wenk, W.Sander. *Angew. Chem., Int. Ed.*, **41**, 2742 (2002)
126. H.F.Bettinger, W.Sander. *J. Am. Chem. Soc.*, **125**, 9726 (2003)
127. M.Winkler, W.Sander. *Angew. Chem. Int. Ed.*, **42**, 502 (2003)
128. W.Sander, D.Grote, S.Kossman, F.Neese. *J. Am. Chem. Soc.*, **130**, 4396 (2008)
129. D.Grote, W.Sander. *J. Org. Chem.*, **74**, 7370 (2009)
130. W.Sander, M.Winkler, B.Cakir, D.Grote, H.F.Bettinger. *J. Org. Chem.*, **72**, 715 (2007)
131. D.Grote, C.Finke, P.Neuhaus, W.Sander. *Eur. J. Org. Chem.*, 3229 (2012)
132. D.Grote, C.Finke, S.Kossmann, F.Neese, W.Sander. *Chem. – Eur. J.*, **16**, 4496 (2010)
133. J.Mieres-Perez, S.Henkel, E.Mendez-Vega, T.Schleif, T.Lohmiller, A. Savitski, W.Sander. *J. Phys. Org. Chem.*, **30**, e3621 (2017)
134. A.Rajca, S.Rajca, S.R.Desai. *J. Am. Chem. Soc.*, **117**, 806 (1995)
135. J.Fujita, Y.Matsuoka, K.Matsuo, M.Tanaka, T.Akita, N.Koga, J.Fujita, T.Akita, H.Iwamura. *Chem. Commun.*, 2393 (1997)
136. A.L.Buchachenko. *Russ. Chem. Rev.*, **59**, 307 (1990)
137. A.Rajca. *Chem. Rev.*, **94**, 871 (1994)
138. N.M.Shishlov. *Russ. Chem. Rev.*, **75**, 863 (2006)
139. D.Gatteschi, R.Sessoli, J.Villain. *Molecular Nanomagnets*. (New York: Oxford University Press, 2006)
140. G.A.Craig, M.Murrie. *Chem. Soc. Rev.*, **44**, 2135 (2015)
141. J.Ferrando-Soria, J.Vallejo, M.Castellano, J.Martinez-Lillo, E.Pardo, J.Cano, I.Castro, F.Lloret, R.Ruiz-Garcia, M.Julve. *Coord. Chem. Rev.*, **339**, 17 (2017)
142. J.M.Frost, K.L.M.Harriman, M.Murugesu. *Chem. Sci.*, **7**, 2470 (2016)
143. L.B.Volodarsky, V.A.Reznikov, V.I.Ovcharenko. *Synthetic Chemistry of Stable Nitroxides*. (Boca Raton, FL: CRC Press, 1994)
144. E.V.Tretyakov, V.I.Ovcharenko. *Russ. Chem. Rev.*, **78**, 971 (2009)
145. A.A.Ovchinnikov. *Theor. Chim. Acta*, **47**, 297 (1978)
146. N.M.Gallagher, A.Olankitwanit, A.Rajca. *J. Org. Chem.*, **80**, 1291 (2015)
147. L.Ratera, J.Veciana. *Chem. Soc. Rev.*, **41**, 303 (2012)
148. A.J.Wingate, B.W.Boudouris. *J. Polym. Sci., Part A: Polym. Chem.*, **54**, 1875 (2016)
149. A.Rajca. *Adv. Phys. Org. Chem.*, **40**, 153 (2005)
150. P.M.Lahti. *Adv. Phys. Org. Chem.*, **45**, 93 (2011)
151. M.Baumgarten. *EPR of Free Radicals in Solids II, Progress in Theoretical Chemistry and Physics*, **25**, 205 (2013)
152. M.Baumgarten. *Mater. Energy*, **10**, 1 (2018)
153. S.Kumar, Y.Kumar, S.Kumar Keshri, P.Mukhopadhyay. *Magnetochemistry*, **2**, 42 (2016)
154. M.S.Platz. *Kinetics and Spectroscopy of Carbenes and Biradicals*. (New York: Plenum, 1990)
155. G.Betrand. *Carbene Chemistry*. (New York: Marcel Dekker, 2002)
156. H.Iwamura. *Proc. Jpn. Acad., Ser. B*, **81**, 233 (2005)
157. W.Sander, G.Bucher, S.Wierlacher. *Chem. Rev.*, **93**, 1583 (1993)
158. H.Iwamura, N.Koga. *Acc.Chem. Res.*, **26**, 346 (1993)
159. D.Daugherty. *Acc. Chem. Res.*, **24**, 88 (1991)
160. M.Abe. *Chem. Rev.*, **113**, 7011 (2013)
161. G.N.Lipunova, N.G.Fedorenko, O.N.Chupakhin. *Russ. Chem. Rev.*, **82**, 701 (2013)
162. J.H.Hall, J.M.Fargher, M.R.Gisler. *J. Am. Chem. Soc.*, **100**, 2029 (1978)
163. E.Wasserman, A.M.Trozzolo, W.A.Yager, R.W.Murray. *J. Chem. Phys.*, **40**, 2408 (1964)
164. A.M.Trozzolo, W.A.Yager, G.W.Griffin, H.Kristinsson, I.Saker. *J. Am. Chem. Soc.*, **89**, 3357 (1967)
165. R.Schmidt, H.-D.Brauer. *Angew. Chem., Int. Ed.*, **10**, 506 (1971)
166. P.Neuhaus, D.Grote, W.Sander. *J. Am. Chem. Soc.*, **130**, 2993 (2008)
167. M.Rule, A.R.Matlin, E.F.Hilinsski, D.A.Doghertt, J.A.Berson. *J. Am. Chem. Soc.*, **101**, 5098 (1979)
168. W.Adam, C.van Barneveld, S.E.Bottle, H.Engert, G.Hanson, H.M.Harrer, C.Heim, W.M.Nau, D.Wang. *J. Am. Chem. Soc.*, **118**, 3974 (1996)
169. A.Rajca, K.Shiraishi, M.Pink, S.Rajca. *J. Am. Chem. Soc.*, **129**, 7232 (2007)
170. A.Olankitwanit, S.Rajca, A.Rajca. *J. Org. Chem.*, **80**, 5035 (2015)
171. A.Rajca, M.Takahashi, M.Pink, G.Spagnol, S.Rajca. *J. Am. Chem. Soc.*, **129**, 10159 (2007)
172. G.Spagnol, K.Shiraishi, S.Rajca, A.Rajca. *Chem. Commun.*, 5047 (2005)
173. A.Rajca, M.Vale, S.Rajca. *J. Am. Chem. Soc.*, **130**, 9099 (2008)
174. R.M.Fico Jr., M.F.Hay, S.Reese, S.Hammond, E.Lambert, M.A.Fox. *J. Org. Chem.*, **64**, 9386 (1999)
175. W.Schlenk, M.Brauns. *Chem. Ber.*, **48**, 661 (1915)
176. K.Hirai, T.Itoh, H.Tomioka. *Chem. Rev.*, **109**, 3275 (2009)
177. M.Kawana, K.Hirai, H.Tomioka, Y.Ohashi. *J. Am. Chem. Soc.*, **129**, 2383 (2007)
178. A.Rajca, A.Olankitwanit, Y.Wang, P.J.Boratynski, M.Pink, S.Rajca. *J. Am. Chem. Soc.*, **135**, 18205 (2013)
179. P.J.Boratynski, M.Pink, S.Rajca, A.Rajca. *Angew. Chem., Int. Ed.*, **49**, 5459 (2010)
180. L.Mahe, A.Izuoka, T.Sugawara. *J. Am. Chem. Soc.*, **114**, 7904 (1992)
181. T.Takayama, T.Mitsumori, M.Kawano, A.Sekine, H.Uekusa, Y.Ohashi, T.Sugawara. *Acta Crystallogr. Sect. B*, **66**, 639 (2010)
182. K.Itoh. *Chem. Phys. Lett.*, **1**, 235 (1967)
183. Y.Teki, I.Fujita, T.Takui, T.Kinoshita, K.Itoh. *J. Am. Chem. Soc.*, **116**, 11499 (1994)
184. A.Isuoka, S.Murata, T.Sugawara, H.Iwamura. *J. Am. Chem. Soc.*, **109**, 2631 (1987)
185. Y.Omokawa, S.Hatano, M.Abe. *J. Phys. Org. Chem.*, **28**, 116 (2015)
186. A.Rajca, S.Utamapanya. *J. Am. Chem. Soc.*, **115**, 2396 (1993)
187. T.Takui, K.Itoh. *Chem. Phys. Lett.*, **19**, 120 (1973)
188. Y.Teki, T.Takui, H.Yagi, K.Itoh, H.Iwamura. *Chem. Phys.*, **83**, 539 (1985)
189. W.Adam, M.Baumgarten, W.Maas. *J. Am. Chem. Soc.*, **122**, 6735 (2000)
190. T.Itoh, K.Hirai, H.Tomioka. *Bull. Chem. Soc. Jpn.*, **80**, 138 (2007)
191. H.Tomioka, M.Hottori, K.Hirai, K.Sato, D.Shiomi, T.Takui, K.Itoh. *J. Am. Chem. Soc.*, **120**, 1106 (1998)
192. Y.Teki, T.Takui, K.Itoh, H.Iwamura, K.Kobayashi. *J. Am. Chem. Soc.*, **105**, 3722 (1983)
193. A.Rajca, S.Utamapanya, S.Thayumanavan. *J. Am. Chem. Soc.*, **114**, 1884 (1992)
194. I.Fujita, Y.Teki, T.Takui, T.Kinoshita, K.Itoh, F.Miko, Y.Sawaki, H.Iwamura, A.Izuoka, T.Sugawara. *J. Am. Chem. Soc.*, **112**, 4074 (1990)
195. N.Nakamura, K.Inoue, H.Iwamura, T.Fujioka, Y.Sawai. *J. Am. Chem. Soc.*, **114**, 1484 (1992)
196. K.Matsuda, N.Nakamura, K.Takahashi, K.Inoue, N.Koga, H.Iwamura. *J. Am. Chem. Soc.*, **117**, 5550 (1995)
197. K.Matsuda, N.Nakamura, K.Inoue, N.Koga, H.Iwamura. *Chem. – Eur. J.*, **2**, 259 (1996)
198. N.Nakamura, K.Inoue, H.Iwamura. *Angew. Chem., Int. Ed.*, **32**, 872 (1993)
199. A.Rajca, J.Wongsriratanakul, S.Rajca. *J. Am. Chem. Soc.*, **126**, 6608 (2004)
200. A.Rajca, J.Wongsriratanakul, S.Rajca. *Science*, **294**, 1503 (2001)
201. U.Banerjee, W.L.Karney, B.S.Ault, A.D.Gudmundsdottir. *Molecules*, **25**, 543 (2020)

202. I.Seghir, N.Nebbache, Y.Meftah, S.E.Hachani, S.Maou. *Acta Chim. Slov.*, **66**, 629 (2019)
203. K.Batra, S.Zahn, T.Heine. *Adv. Theory Simulat.*, **3**, 1900192 (2020)
204. D.Ganyushin, N.Gilka, P.R.Taylor, C.M.Marian, F.Neese. *J. Chem. Phys.*, **132**, 144111 (2010)
205. A.V.Akimov, Yu.S.Ganushevich, D.V.Korchagin, V.A.Miluykov, E.Y.Misochko. *Angew. Chem., Int. Ed.*, **56**, 7944 (2017)
206. K.Sato, Ph.D. Thesis. Osaka City University, Osaka, Japan, 1994
207. M.Griffin, A.Muys, C.Noble, D.Wang, C.Eldershaw, K.E.Gates, K.Burrage, G.R.Hanson. *Mol. Phys. Rep.*, **26**, 60 (1999)
208. S.Mossin, H.Weihe, A.-L.Barra. *J. Am. Chem. Soc.*, **124**, 8764 (2002)
209. R.Sessoli, D.Gatteschi, A.Caneschi, M.A.Novak. *Nature (London)*, **365**, 141 (1993)
210. M.D.Jenkins, Y.Duan, B.Diosdado, J.J.Garcia-Ripoll, A.Gaita-Ariño, C.Giménz-Saiz, P.J.Alonso, E.Coronado, F.Luis. *Phys. Rev. B*, **95**, 064423 (2017)
211. K.Sugisaki, S.Yamamoto, S.Nakazawa, K.Toyota, K.Sato, D.Shiomi, T.Takui. *J. Phys. Chem. A*, **120**, 6459 (2016)
212. K.Sugisaki, S.Nakazawa, K.Toyota, K.Sato, D.Shiomi, T.Takui. *ACS Cent. Sci.*, **5**, 167 (2019)
213. K.Sugisaki, S.Nakazawa, K.Toyota, K.Sato, D.Shiomi, T.Takui. *Phys. Chem. Chem. Phys.*, **21**, 15356 (2019)
214. K.Sugisaki, S.Yamamoto, S.Nakazawa, K.Toyota, K.Sato, D.Shiomi, T.Takui. *Chem. Phys. Lett.: X*, **1**, 100002 (2019)